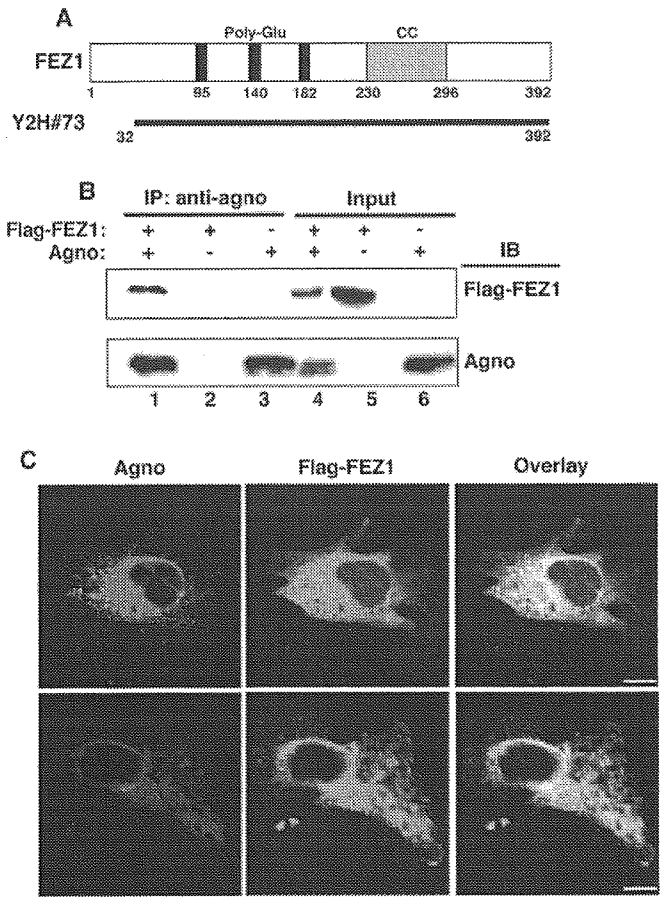

FIG. 1. **Interaction of JCV agnoprotein and FEZ1.** *A*, predicted structural organization of human FEZ1. FEZ1 contains three poly-Glu regions (*black rectangles*) and a CC domain (*gray rectangle*). The *black bar* indicates a FEZ1 clone (Y2H #73) isolated from a human brain cDNA library by a yeast two-hybrid assay with full-length JCV agnoprotein as the bait. *B*, interaction of agnoprotein with FEZ1 in mammalian cells. 293AG cells were transfected with pFLAG-FEZ1 (*lanes 1, 2, 4,* and *5*) or with the corresponding empty vector (*lanes 3* and *6*), and were subsequently incubated in the absence (*lanes 2* and *5*) or presence (*lanes 1, 3, 4,* and *6*) of Dox for 24 h. Cell lysates were then subjected to immunoprecipitation (*IP*) with antibodies to agnoprotein (*anti-agno*), and the resulting precipitates were subjected to immunoblot analysis (*IB*) with antibodies to FLAG or to agnoprotein, as indicated (*lanes 1–3*). A portion of cell lysates corresponding to 2% of the input for immunoprecipitation was also subjected directly to immunoblot analysis with the same antibodies (*lanes 4–6*). *C*, intracellular localization of recombinant agnoprotein and FLAG-FEZ1. HEK293 cells were transfected with pFLAG-FEZ1 and pcDNA4HisMax-agnoprotein. Forty-eight hours after transfection, the cells were stained with antibodies to agnoprotein (*red, left*) and to FLAG (*green, center*). The merged fluorescence images (*Overlay, right*) are also shown. *Scale bars*, 10 μm.

nocodazole (*lanes 2* and *7*) or 20 μM Taxol (*lanes 3* and *8*) or 40 μM nocodazole-treated microtubules (*lanes 4* and *9*) or 20 μM Taxol-treated microtubules (*lane 5* and *10*). In the absence of polymerized microtubules, agnoprotein remains in the supernatant fraction (*lanes 1–3*). Only small amounts of agnoprotein were detected in the sedimented fraction in the presence of nocodazole-treated microtubules (*lane 9*), whereas a significant amount of agnoprotein associated with microtubule pellets in the presence of Taxol-polymerized microtubules (*lane 10*). These results demonstrate that agnoprotein binds directly to microtubules. To examine if agnoprotein colocalizes specifically with microtubules, JCV-infected cells (JCI cells) were treated with either cytochalasin D, which specifically depolymerizes actin fibers, or nocodazole, which depolymerizes microtubules (Fig. 2*E*). In cells treated with Me_2SO or cytochalasin D, agnoprotein was still localized in the perinuclear region and cytoplasm. In cells treated with nocodazole, however, agnoprotein was found in aggregates dispersed throughout the remainder of the cell. These observations suggest that agnoprotein colocalizes specifically with microtubules.

Agnoprotein-induced Dissociation of FEZ1 from Microtubules—We next examined whether a GST fusion protein of full-length FEZ1 interacted with microtubules in the microtubule cosedimentation assay. GST-FEZ1, but not GST, was detected in the sedimented fraction in the presence of polymerized microtubules (Fig. 3*A*). In addition, both α-tubulin and agnoprotein were detected in immunoprecipitates prepared with antibodies to GFP from lysates of Dox-treated 293AG cells expressing a FEZ1-GFP fusion protein (Fig. 3*B*). Together, these data suggested that FEZ1 directly interacts with microtubules.

To examine whether agnoprotein affects the interaction of FEZ1 with microtubules, we performed the microtubule cosedimentation assay with lysates of 293AG cells stably expressing FEZ1-GFP. The expression level of agnoprotein in the cells was varied by their incubation with Dox for 0, 3, 6, 12, or 24 h. The amount of FEZ1-GFP that cosedimented with microtubules decreased as the expression level of agnoprotein increased (Fig. 3*C*). Conversely, the amount of agnoprotein that precipitated with microtubules increased in a concentration-dependent manner. However, the amount of MAP2 that cosedimented with microtubules did not change. These observations suggested that agnoprotein induces the dissociation of FEZ1 from microtubules, and that competition is specific between agnoprotein and FEZ1.

Regions of FEZ1 That Mediate Interaction with Microtubules and Agnoprotein—To identify the region of FEZ1 that mediates its interaction with agnoprotein, we constructed a series of deletion mutants of FEZ1 as GST fusion proteins (Fig. 4, *A* and *B*) and subjected them to GST precipitation assays. The deletion mutants of FEZ1 fused to GST were incubated with purified the histidine-tagged agnoprotein (His-Agno) expressed in insect cells and then precipitated with glutathione-Sepharose beads. Immunoblot analysis of bead-bound proteins revealed that wild-type FEZ1 and the deletion mutant of FEZ1 containing residues 192–392 (C192) interacted with agnoprotein to similar extents, whereas the deletion mutant of FEZ1 containing residues 163–296 (N296) precipitated progressively smaller amounts of agnoprotein, and no binding was observed with the COOH-terminal deletion mutant containing residues 1–191 (N191) and an NH_2-terminal deletion mutant containing residues 297–392 (C297) (Fig. 4*C*). These observations suggested that agnoprotein binds directly to FEZ1, and the CC domain of FEZ1 is important for the association with agnoprotein.

We next attempted to delineate the region of FEZ1 responsible for association with microtubules. The deletion mutants of FEZ1 fused to GST were subjected to a microtubules cosedimentation assay. The FEZ1 C192 and FEZ1 C297 mutants retained the ability to bind to microtubules (Fig. 4*D*). In contrast, the FEZ1 N191 mutant failed to interact with microtubules. The FEZ1 N296 mutant detected in sedimented fraction in the absence of microtubules as well as presence of microtubules, showing that the FEZ1 N296 mutant could sediment by itself independently with microtubules. These results suggested that the COOH-terminal region (residues 297–392) of FEZ1 contribute to the interaction with microtubules.

Thus, we have demonstrated that the binding regions of agnoprotein and microtubules with FEZ1 did not overlap each other. To further investigate the mechanism how agnoprotein disrupts the interaction between FEZ1 and microtubules, we performed a GST precipitation assay using GST-fused FEZ1 proteins and cell lysates from the agnoprotein-inducible cell line (293AG cells). This demonstrated that precipitated α-tu-

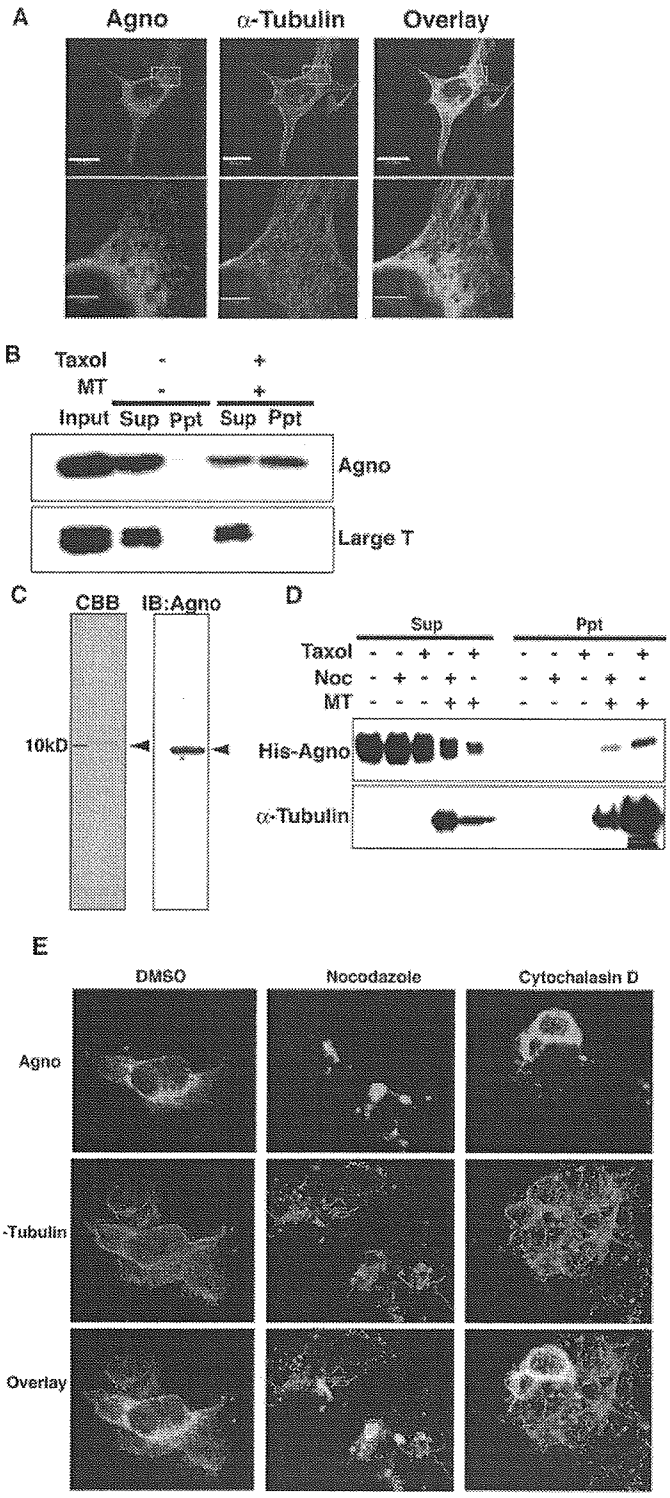

FIG. 2. **Interaction between JCV agnoprotein and microtubules.** *A*, intracellular localization of agnoprotein (*red*, *left*) and α-tubulin (*green*, *center*) in JCV-infected SVG-A cells. The merged fluorescence images (*Overlay*, *right*) are also shown. The cells were examined 7 days after inoculation with JCV (1,000 hemagglutination units per 1×10^6 cells). *Enlarged dotted rectangles* of the images are represented in the *lower panels*. *Scale bars*, 20 μm (*upper panels*) and 5 μm (*lower panels*). *B*, microtubule cosedimentation assay with a lysate of JCV-infected SVG-A cells. Cell lysate was incubated in the absence (−) or presence (+) of microtubules (*Mt*) and Taxol (*Taxol*), after which the precipitates (*Ppt*) and supernatants (*Sup*) obtained by centrifugation of the incubation mixtures were subjected to immunoblot analysis with antibodies to agnoprotein and to JCV large T antigen. A portion of the cell lysate corresponding to 10% of the input to the sedimentation assay was also subjected directly to immunoblot analysis with the same antibodies. *C*, the purified histidine-tagged agnoprotein (*arrowhead*).

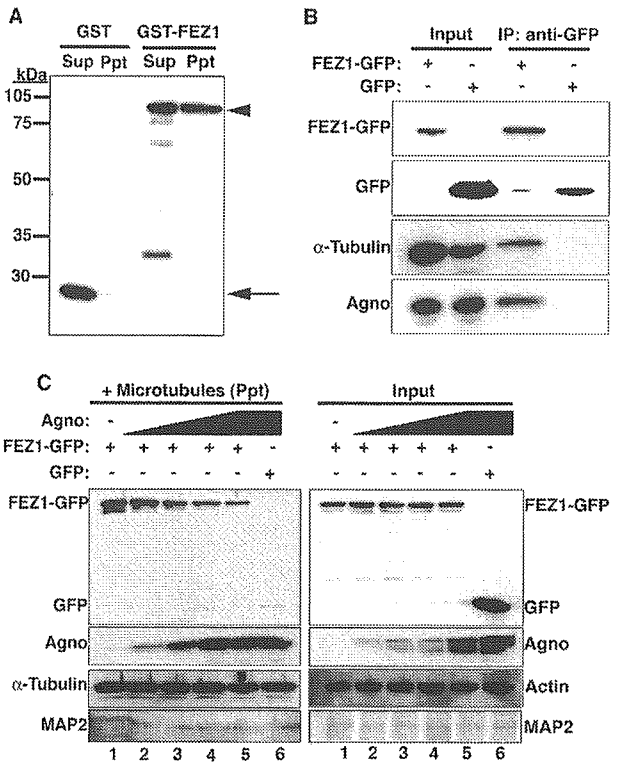

FIG. 3. **Agnoprotein-sensitive interaction of FEZ1 with microtubules.** *A*, microtubule cosedimentation assay performed with GST or GST-FEZ1. The recombinant proteins were incubated with microtubules, after which the precipitates and supernatants of the incubation mixtures were subjected to immunoblot analysis with antibodies to GST. The positions of GST-FEZ1 (*arrowhead*) and GST (*arrow*) are indicated. *B*, coprecipitation of α-tubulin and agnoprotein with FEZ1-GFP. 293AG cells stably expressing FEZ1-GFP or GFP were incubated with Dox (for 24 h), lysed, and subjected to immunoprecipitation with antibodies to GFP, and the resulting precipitates were subjected to immunoblot analysis with antibodies to GFP, to α-tubulin, and to agnoprotein. A portion of the cell lysates corresponding to 5% of the input for immunoprecipitation was also subjected directly to immunoblot analysis with the same antibodies. *C*, agnoprotein-induced dissociation of FEZ1 from microtubules. 293AG cells stably expressing FEZ1-GFP (*lanes 1–5*) or GFP (*lanes 6*) were incubated with Dox for 0 h (*lanes 1*), 3 h (*lanes 2*), 6 h (*lanes 3*), 12 h (*lanes 4*), or 24 h (*lanes 5* and *6*) and were then subjected to the microtubule cosedimentation assay. The microtubule precipitates (*left panel*) as well as a portion of the cell lysates corresponding to 10% of the input to the sedimentation assay (*right panel*) were subjected to immunoblot analysis with antibodies to GFP, to agnoprotein, to MAP2, and either to α-tubulin or to actin.

bulin with wild type FEZ1 or FEZ1 C192 mutant were remarkably attenuated in the presence of agnoprotein; however, precipitated α-tubulin with FEZ1 C297 mutant lacking the agnoprotein binding site was not altered even in the presence of

20 μl of sample was subjected to SDS-PAGE and CBB staining (*left panel*), immunoblot analysis (*right panel*). *D*, microtubule cosedimentation assay with the purified histidine-tagged agnoprotein (*His-Agno*). His-Agno was incubated in the absence (*lanes 1* and *6*) or presence of 40 μM nocodazole (*lanes 2* and *7*) or 20 μM Taxol (*lanes 3* and *8*) or 40 μM nocodazole-treated microtubules (*lanes 4* and *9*) or 20 μM Taxol-treated microtubules (*lanes 5* and *10*), after which the precipitates (*Ppt*) and supernatants (*Sup*) obtained by centrifugation of the incubation mixtures were subjected to immunoblot analysis with antibodies to agnoprotein and to α-tubulin. *E*, effect of nocodazole and cytochalasin D on the localization of agnoprotein in JCV-infected cells. JCI cells in absence of drugs (Me_2SO (*DMSO*), *left*) or treated with 4 μM nocodazole (*center*) or 0.5 μM cytochalasin D (*right*) were incubated for 2 h at 37 °C. The cells were extracted with 0.2% saponin, fixed, and analyzed by double immunofluorescence with anti-agnoprotein antibody (*green*, *upper*) and anti-α-tubulin antibody (*red*, *middle*). The merged fluorescence images (*Overlay*) are also shown.

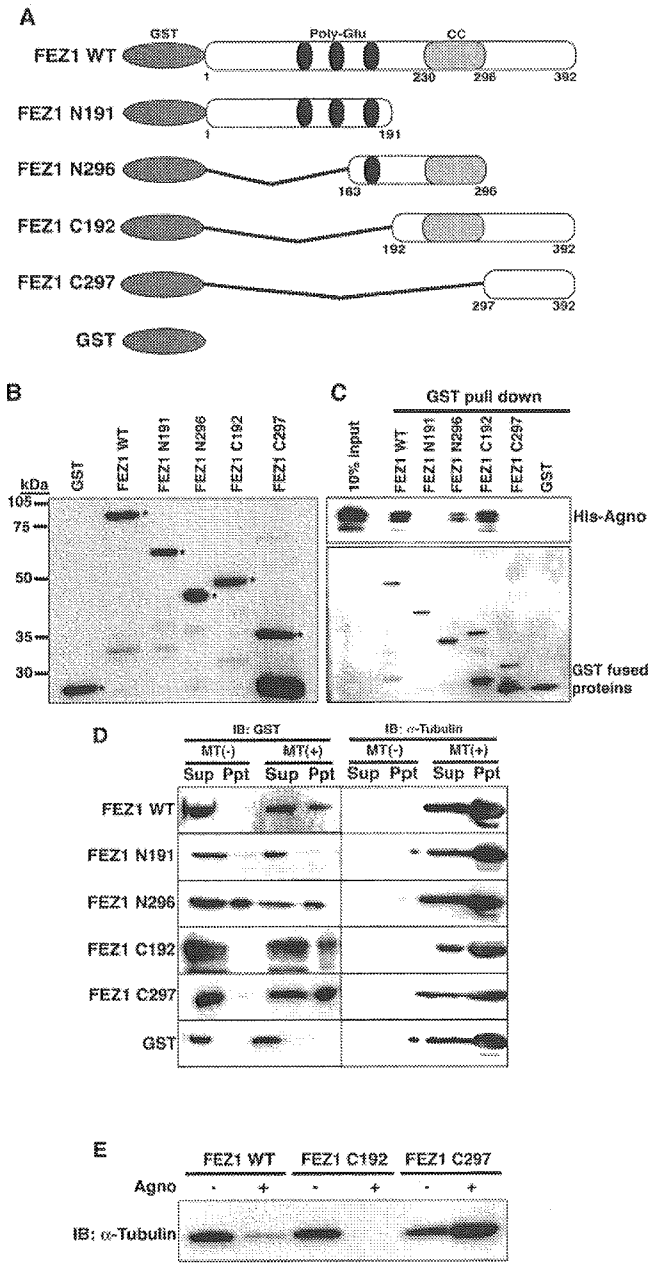

FIG. 4. **Delineation of the regions of FEZ1 that mediate interaction with microtubules and agnoprotein.** *A*, schematic representation of GST fusion constructs of wild-type (*WT*) FEZ1 and various FEZ1 deletion mutants. *B*, immunoblot analysis with antibodies to GST of the GST fusion proteins of FEZ1 deletion mutants purified from bacteria. *Asterisks* indicate the mature recombinant proteins. *C*, *in vitro* precipitation assay with the GST-FEZ1 deletion mutants and His-Agno. After incubation with His-Agno, the GST fusion proteins were precipitated with glutathione-Sepharose and bead-bound proteins were subjected to immunoblot analysis with antibodies to agnoprotein (*upper panel*) or to GST (*lower panel*). A portion of His-Agno corresponding to 10% of the input to the binding assay was also subjected directly to immunoblot analysis. *D*, microtubule cosedimentation assay performed with the GST fusion proteins of FEZ1 deletion mutants. The supernatant and precipitate fractions were subjected to immunoblot analysis with antibodies to GST. *E*, GST precipitation assay using GST-fused WT and mutant FEZ1 proteins and cell lysates from the agnoprotein-inducible cell line (293AG cells). After incubation with cell lysates, the GST fusion proteins were precipitated with glutathione-Sepharose, and bead-bound proteins were subjected to immunoblot analysis with antibodies to α-tubulin.

agnoprotein (Fig. 4*E*). These results suggested that the interaction of agnoprotein with FEZ1 at the CC domain is essential for disruption of interaction between microtubules and FEZ1 at the COOH-terminal region.

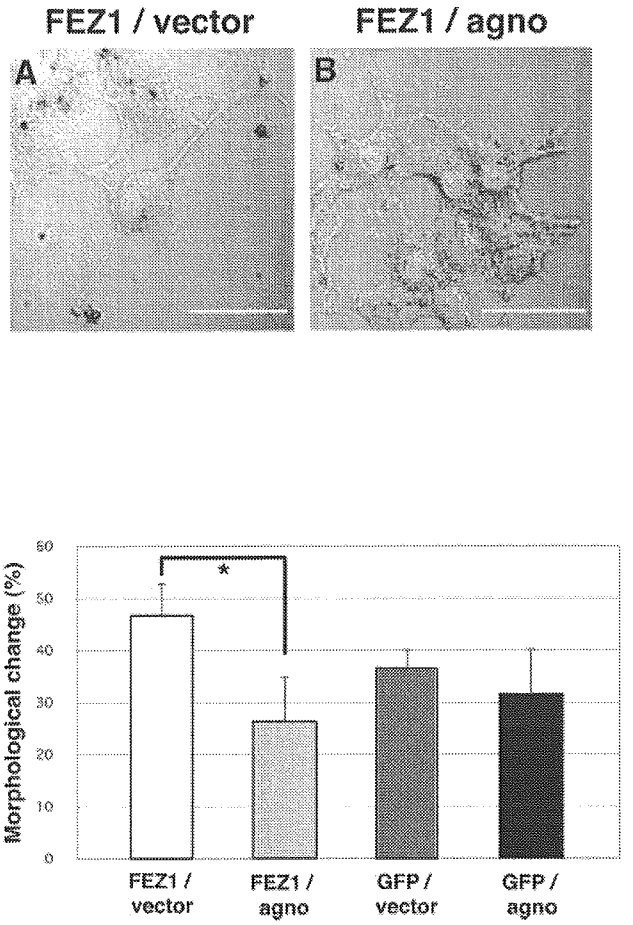

FIG. 5. **Agnoprotein-induced inhibition of the promotion of neurite outgrowth by FEZ1 in PC12 cells.** *A* and *B*, representative morphology of NGF-treated PC12 cells expressing FEZ1-GFP in the absence or presence of agnoprotein, respectively. The nuclei of transfected cells are colored *red* by DsRed. *Scale bars*, 50 μm. *C*, PC12 cells stably expressing GFP or FEZ1-GFP were transfected with the bicistronic expression vector pERedNLS-agno (*agno*) or pERedNLS (*vector*) and subsequently exposed to NGF. The cells were examined by fluorescence microscopy, and those that had been successfully transfected were identified by their DsRed-positive nuclei. The percentage of cells that underwent a morphological change, characterized in part by flattening of the cell body and extension of neurites with a length at least twice the diameter of the soma, was determined by evaluation of >300 cells with DsRed-positive nuclei. Data are means ± S.D. of values from three independent experiments. *, $p < 0.05$ for the indicated comparison (Student's *t* test).

Inhibition by Agnoprotein of the Promotion of Neurite Outgrowth by FEZ1 in PC12 Cells—FEZ1 has been implicated in axonal outgrowth and fasciculation (23) and promotes neurite extension in rat pheochromocytoma PC12 cells (37). We have now shown that FEZ1 associates with microtubules, and cytoskeletal filaments, including microtubules, are the final common target of various signaling cascades that influence development of the growth cone and neurite extension (39). To examine the possible effect of agnoprotein on the promotion of neurite outgrowth by FEZ1 in PC12 cells, which cease proliferation and begin to extend neurites in response to stimulation with NGF, we transfected PC12 cells that stably express FEZ1-GFP or GFP with pERedNLS-agno or the empty vector. Agnoprotein-expressing cells were thus labeled by expression of DsRed in the nucleus. Agnoprotein significantly inhibited neurite extension in NGF-treated cells that expressed FEZ1-GFP, but it had no effect on neurite outgrowth in NGF-treated cells expressing GFP (Fig. 5). These results suggested that agnoprotein inhibits the promotion of neurite outgrowth by FEZ1 in PC12 cells.

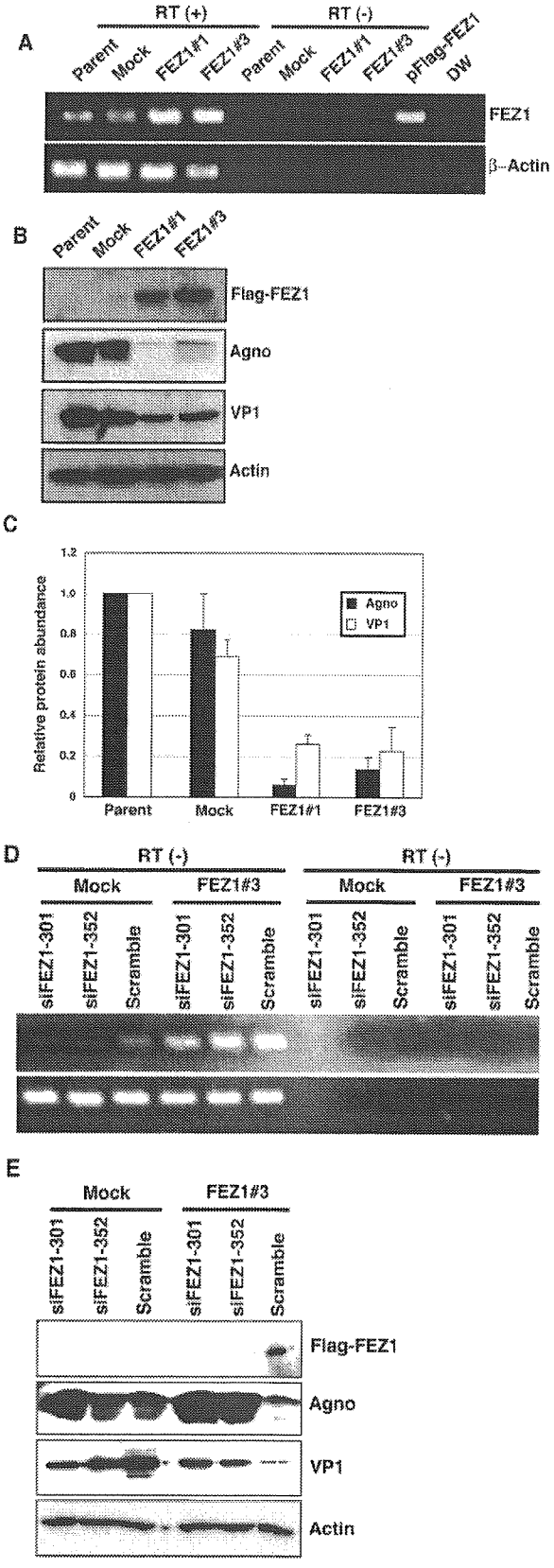

FIG. 6. **Suppression by FEZ1 of JCV protein expression in SVG-A cells inoculated with JCV.** *A*, RT-PCR analysis of FEZ1 mRNA (and β-actin mRNA) in SVG-A cells either stably expressing FLAG-FEZ1 (*FEZ1#1* and *FEZ1#3*) or stably transfected with the empty vector (*Mock*) as well as in parental SVG-A cells. The analysis was performed with or without RT. PCR controls were also performed with pFLAG-FEZ1 or distilled water (*DW*) as the template. *B*, immunoblot analysis of FEZ1#1, FEZ1#3, mock-transfected, and parental SVG-A cells lysed 7 days after inoculation with JCV (1000 hemagglutination units per 5 × 10^5 cells). The analysis was performed with antibodies to FLAG, to agnoprotein, to VP1, and to actin. *C*, the intensity of the immunoreactive bands corresponding to agnoprotein and VP1 in blots similar to that shown in *B* was quantified with an image analyzer and expressed relative to the values for parental SVG-A cells. Data are means ± S.D. of values from three independent experiments. *D*, RT-PCR analysis of FEZ1 mRNA (and β-actin mRNA) in FEZ1#3 cells or Mock cells transfected with siRNA against FEZ1 (*siFEZ1–301* and *siFEZ1–352*) or Scramble siRNA. *E*, immunoblot analysis of FEZ1#3 and mock-transfected SVG-A cells lysed 4 days after transfection with siRNA. These cells were inoculated with JCV (1000 hemagglutination units per 1 × 10^5 cells) on the preceding day of transfection. The analysis was performed with antibodies to FLAG, to agnoprotein, to VP1, and to actin.

Inhibition by FEZ1 of JCV Protein Expression in SVG-A Cells Inoculated with JCV—To examine the possible effects of FEZ1 on JCV infection in SVG-A cells, we established SVG-A cells that stably express FLAG-FEZ1. Given the lack of antibodies to FEZ1, we examined total (endogenous plus exogenous) FEZ1 expression by RT-PCR. The amount of FEZ1 mRNA in cells stably expressing FLAG-FEZ1 (FEZ1#1 and FEZ1#3 lines) was higher than that apparent in parental SVG-A cells or in cells stably transfected with the empty vector (Fig. 6*A*). The abundance of JCV agnoprotein and VP1 was markedly reduced in the cells expressing FLAG-FEZ1 compared with that apparent in control cells after inoculation with JCV (Fig. 6, *B* and *C*). To confirm if the effect for JCV infection in FLAG-FEZ1-expressing SVG-A cells depends on the expression of FEZ1, we used stealth siRNA (Invitrogen) to reduce the expression of FEZ1. At 24-h post inoculation of JCV, siRNAs (siFEZ1–301, siFEZ1–352, and Scramble) were transfected. The cells were harvested and analyzed by immunoblot at 96-h post transfection. The amount of FEZ1 mRNA in cells transfected with siFEZ1–301 or siFEZ1–352 siRNA was lower than that transfected with Scramble siRNAs (Fig. 6*D*). In the cells expressing FLAG-FEZ1, the abundance of JCV agnoprotein and VP1 was markedly increased in the cells transfected with siRNA to FEZ1 compared with Scramble siRNA. On the other hand, no difference was shown with cells transfected with siRNA to FEZ1 and Scramble in the cells stably transfected with the empty vector (Fig. 6*E*). FEZ1 thus suppressed the expression of JCV proteins in SVG-A cells. We also examined the transcriptional activity of JCV promoters in these various cell lines with a luciferase reporter assay but found no effect of FLAG-FEZ1 (data not shown).

Inhibition by FEZ1 of JCV Propagation in SVG-A Cells—Finally, we examined JCV-inoculated SVG-A cell lines by immunocytofluorescence analysis with antibodies to VP1. The number of VP1-positive cells did not differ significantly between either FEZ1#1 or FEZ1#3 cells and mock-transfected cells 3 days after inoculation (Fig. 7*A*). In contrast, the proportion of VP1-positive cells was significantly smaller for FEZ1#1 or FEZ1#3 cells than for mock-transfected cells 7 days after inoculation (Fig. 7), suggesting that FEZ1 suppressed the propagation of JCV in SVG-A cells. VP1 immunoreactivity was detected in the nucleus and cytoplasm of both parental and mock-transfected cells but was restricted to the nucleus in FEZ1#1 and FEZ1#3 cells 7 days after inoculation (Fig. 7*B*). These data suggested that FEZ1 suppressed the translocation of VP1 from the nucleus to the cytoplasm. We also analyzed the JCV inoculated cells by electron microscopy. This revealed that virion formation was intact in FEZ1-overexpressing cells (data not shown).

DISCUSSION

In the present study, we have identified FEZ1 as a binding partner of JCV agnoprotein. FEZ1 is a brain-specific protein and a mammalian homolog of *C. elegans* UNC-76 (23). Agno-

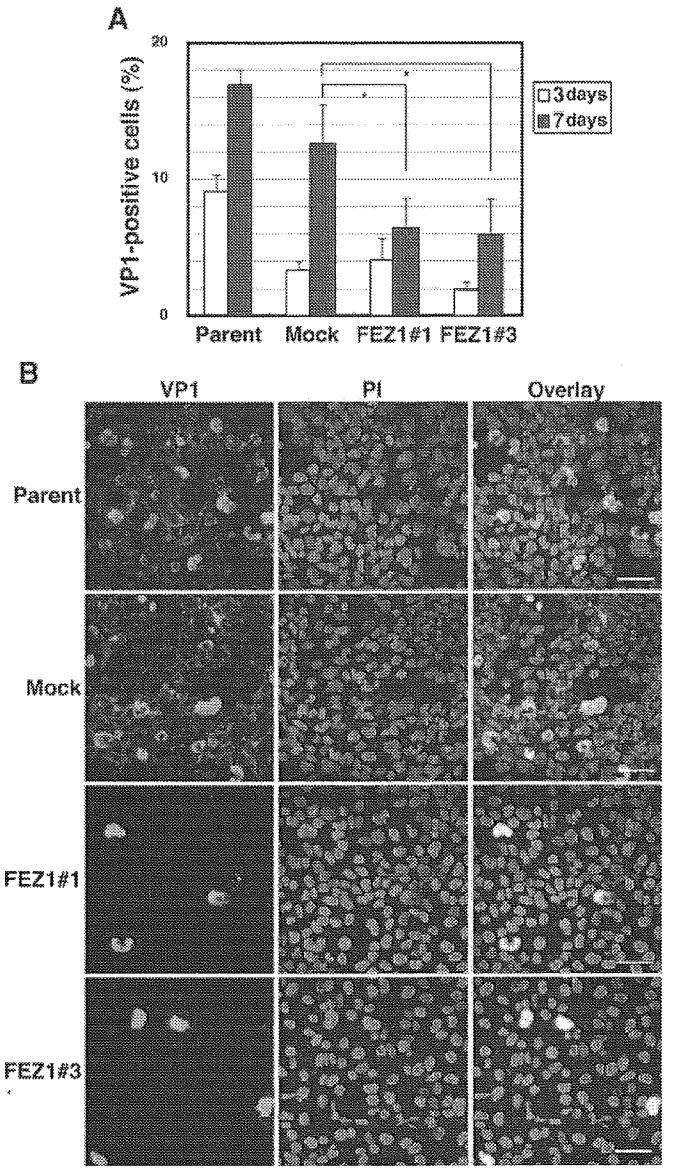

FIG. 7. **Suppression by FEZ1 of JCV propagation in SVG-A cells.** *A*, the proportion of VP1-positive cells among FEZ1#1, FEZ1#3, mock-transfected, and parental SVG-A cells determined by immunofluorescence analysis 3 and 7 days after inoculation with JCV as in Fig. 6. Data are means ± S.D. of values from three independent experiments. *, $p < 0.05$ for the indicated comparisons (Student's *t* test). *B*, immunostaining with antibodies to VP1 (*green*) of the indicated SVG-A cell lines at 7 days after inoculation with JCV. Cell nuclei were counterstained *red*. *Scale bars*, 50 μm.

protein interacted with FEZ1 in both yeast and mammalian cells and colocalized with both FEZ1 and microtubules in the perinuclear region of mammalian cells. We previously showed that agnoprotein colocalizes with microtubules (38), and we here confirmed the binding of agnoprotein to microtubules with a microtubule cosedimentation assay. Microtubules are a major component of the cytoskeleton in growing axons, and, together with their associated molecules, they play an important role in axon outgrowth (39). We have now shown that FEZ1, which promotes axon outgrowth in PC12 cells (37), also binds to microtubules in the microtubule cosedimentation assay and that the interaction between FEZ1 and microtubules is disrupted by agnoprotein. Regions of FEZ1 that mediate interaction with microtubules and agnoprotein are not the same, and the binding of agnoprotein with the CC domain of FEZ1 plays a pivotal role in disruption of interaction between microtubules and FEZ1. These results suggest that the interaction of agnoprotein with FEZ1 might lead to some conformational changes in the COOH-terminal region of FEZ1, resulting in lost of its ability to combine with microtubules.

The promotion of neurite outgrowth by FEZ1 in PC12 cells was also inhibited by agnoprotein. These results suggest that FEZ1 might promote neurite extension through interaction with microtubules and that this interaction is sensitive to agnoprotein. Overexpression of FEZ1 in human glial cells inhibited the production of JCV agnoprotein and VP1 without affecting transcription from JCV promoters. Although the number of JCV-infected cells did not differ between SVG-A cells stably expressing FEZ1 and control cells at 3 days after inoculation with JCV, the proportion of VP1-positive cells was markedly reduced by FEZ1 overexpression at 7 days. These results suggest that overexpression of FEZ1 influenced the late phase of JCV infection but did not affect the early phase, including the attachment of JCV to cells, its entry into the cytoplasm, and transcription of the JCV genome. Whereas VP1 was present in both the nucleus and cytoplasm of control cells at 7 days after inoculation with JCV, it was restricted to the nucleus of cells overexpressing FEZ1. Given that the antibodies to VP1 used for these experiments recognize both VP1 monomers and mature virus particles, our results suggest that both VP1 monomers and mature JCV virions were restricted to the nucleus of cells stably expressing FEZ1. A mutational analysis of SV40 agnoprotein similarly showed that this protein plays an important role in the release of progeny virions from infected cells and in viral propagation (14–16). The transport of progeny virions of SV40 from the nucleus to the cell surface depends on intracytoplasmic vesicular transport (40). We have detected JCV virions both in the cytoplasm of infected cells and in the surrounding extracellular space in the apparent absence of disruption of the cell membrane both in progressive multifocal leukoencephalopathy lesions and in cell cultures (19). These observations indicate that JCV virions might be released from host cells by a specific mechanism and that FEZ1 might inhibit JCV release from infected human cells.

UNC-76 of *Drosophila*, which is a homolog of FEZ1, binds specifically to the tail domain of kinesin heavy chain in the yeast two-hybrid system and copurification assays. Furthermore, immunostaining and genetic analyses have demonstrated that UNC-76 function is required for axonal transport in the *Drosophila* nervous system (41). Interestingly, we observed that FEZ1 interacted with KIF3A that is a member of KIF3 family by immunoprecipitation assay (data not shown). These observations thus suggest that UNC-76 and FEZ1 play an essential role in kinesin-mediated transport pathways. Kinesin is a plus end-directed microtubule motor that facilitates the movement of vesicles, messenger ribonucleoproteins, and organelles. It was first identified in squid axoplasm as a protein that facilitates ATP-dependent vesicle movement along microtubules (42, 43). Subsequent molecular, genetic, and biochemical studies have shown that kinesin is required for intracellular transport in eukaryotes in many cellular contexts (44–46).

The requirement for kinesin-based transport is especially prominent in polarized cells such as neurons. The polarity complex comprised of PAR3, PAR6, and atypical protein kinase C (PKC) contributes to polarity determination in many tissues and cells (47, 48). FEZ1 was also identified in a yeast two-hybrid assay for proteins that bind the regulatory domain of the rat atypical PKC isoform PKCζ (37). Whereas nonphosphorylated FEZ1 is associated with both cytosolic and membrane fractions of COS-7 cells, its phosphorylation by PKCζ induces the redistribution of membrane-bound FEZ1 to the cytosol. In addition, the phosphorylation of FEZ1 by PKCζ stimulates

neurite outgrowth in PC12 cells. These observations suggest that FEZ1, like UNC-76, might associate with kinesin and is essential for PKCζ-dependent neuronal differentiation.

FEZ1 also interacts in neural cells with the protein Disrupted-In-Schizophrenia 1, which was identified as the product of a gene disrupted by a (1;11)(q42.1;q14.3) chromosomal translocation that segregates with schizophrenia in a Scottish family. Furthermore, interaction of Disrupted-In-Schizophrenia 1 and FEZ1 appears to take place on or near the actin cytoskeleton and is up-regulated during neurite outgrowth (49).

The actin and tubulin cytoskeletons are a final common target of many signaling cascades that influence neuronal development (39), and cytoskeletal dynamics and polarized axonal transport appear to be closely related (50, 51). Our observation that FEZ1 associates with microtubules, combined with its possible interaction with kinesin and the previous finding that it promotes neurite outgrowth, suggest that FEZ1 may play a key role downstream of atypical PKC and the polarity complex in the regulation of vesicle trafficking that contributes to neurite extension.

Although the release of mature progeny virions of SV40 and JCV assembled in the nucleus has been thought to occur through disintegration or rupture of infected cells, these viruses do not encode an enzyme that is able to cause cell lysis. In addition, progeny virions of SV40 have been shown to be transported from the nucleus to the cell surface in a manner dependent on vesicular transport (40). The tegument protein US11 of herpes simplex virus, another DNA virus, interacts with conventional kinesin heavy chain, and this interaction has been thought to be important for anterograde transport of nonenveloped nucleocapsids in axons (52). The transport and release of large numbers of virus particles are undesirable for host cells. It is thus possible that FEZ1 serves a potentially protective function in JCV-infected cells by inhibiting the release of progeny virions. Interestingly, expression of FEZ1 in JCV-permissible cells such as SVG-A cells or IMR-32 cells is much less than nonpermissible neuronal cells (53) such as SH-SY5Y cells (data not shown). This suggests that expression levels of FEZ1 might be a factor that determines JCV tissue specificity. Conversely, the viral agnoprotein may inhibit the physiological function of FEZ1 by inducing its dissociation from microtubules, thereby promoting the effective transmission of progeny viruses.

Acknowledgments—We thank M. Sato and S. Nakagaki for expert technical assistance and Dr. W. W. Hall, Dr. C. Henmi, Y. Makino, and T. Aketagawa for their valuable suggestions.

REFERENCES

1. Frisque, R. J., Bream, G. L., and Cannella, M. T. (1984) *J. Virol.* **51,** 458–469
2. Safak, M., Gallia, G. L., Ansari, S. A., and Khalili, K. (1999) *J. Virol.* **73,** 10146–10157
3. Safak, M., Gallia, G. L., and Khalili, K. (1999) *Mol. Cell. Biol.* **19,** 2712–2723
4. Gallia, G. L., Safak, M., and Khalili, K. (1998) *J. Biol. Chem.* **273,** 32662–32669
5. Major, E. O., Amemiya, K., Tornatore, C. S., Houff, S. A., and Berger, J. R. (1992) *Clin. Microbiol. Rev.* **5,** 49–73
6. Safak, M., Barrucco, R., Darbinyan, A., Okada, Y., Nagashima, K., and Khalili, K. (2001) *J. Virol.* **75,** 1476–1486
7. Cohen, E. A., Subbramanian, R. A., and Gottlinger, H. G. (1996) *Curr. Top. Microbiol. Immunol.* **214,** 219–235
8. Cullen, B. R. (1998) *Cell* **93,** 685–692
9. Michaud, G., Zachary, A., Rao, V. B., and Black, L. W. (1989) *J. Mol. Biol.* **209,** 667–681
10. Terwilliger, E. F., Cohen, E. A., Lu, Y. C., Sodroski, J. G., and Haseltine, W. A. (1989) *Proc. Natl. Acad. Sci. U. S. A.* **86,** 5163–5167
11. Strebel, K., Klimkait, T., Maldarelli, F., and Martin, M. A. (1989) *J. Virol.* **63,** 3784–3791
12. Harris, M. (1999) *Curr. Biol.* **9,** R459–R461
13. Hou-Jong, M. H., Larsen, S. H., and Roman, A. (1987) *J. Virol.* **61,** 937–939
14. Resnick, J., and Shenk, T. (1986) *J. Virol.* **60,** 1098–1106
15. Carswell, S., Resnick, J., and Alwine, J. C. (1986) *J. Virol.* **60,** 415–422
16. Carswell, S., and Alwine, J. C. (1986) *J. Virol.* **60,** 1055–1061
17. Ressetar, H. G., Walker, D. L., Webster, H. D., Braun, D. G., and Stoner, G. L. (1990) *Lab. Invest.* **62,** 287–296
18. Shishido-Hara, Y., Hara, Y., Larson, T., Yasui, K., Nagashima, K., and Stoner, G. L. (2000) *J. Virol.* **74,** 1840–1853
19. Okada, Y., Sawa, H., Endo, S., Orba, Y., Umemura, T., Nishihara, H., Stan, A. C., Tanaka, S., Takahashi, H., and Nagashima, K. (2002) *Acta Neuropathol. (Berl.)* **104,** 130–136
20. Nomura, S., Khoury, G., and Jay, G. (1983) *J. Virol.* **45,** 428–433
21. Okada, Y., Endo, S., Takahashi, H., Sawa, H., Umemura, T., and Nagashima, K. (2001) *J. Neurovirol.* **7,** 302–306
22. Orba, Y., Sawa, H., Iwata, H., Tanaka, S., and Nagashima, K. (2004) *J. Virol.* **78,** 7270–7273
23. Bloom, L., and Horvitz, H. R. (1997) *Proc. Natl. Acad. Sci. U. S. A.* **94,** 3414–3419
24. Tokui, M., Takei, I., Tashiro, F., Shimada, A., Kasuga, A., Ishii, M., Ishii, T., Takatsu, K., Saruta, T., and Miyazaki, J. (1997) *Biochem. Biophys. Res. Commun.* **233,** 527–531
25. Ashok, A., and Atwood, W. J. (2003) *J. Virol.* **77,** 1347–1356
26. Nukuzuma, S., Yogo, Y., Guo, J., Nukuzuma, C., Itoh, S., Shinohara, T., and Nagashima, K. (1995) *J. Med. Virol.* **47,** 370–377
27. Fujita, T., Ikuta, J., Hamada, J., Okajima, T., Tatematsu, K., Tanizawa, K., and Kuroda, S. (2004) *Biochem. Biophys. Res. Commun.* **313,** 738–744
28. Suzuki, S., Sawa, H., Komagome, R., Orba, Y., Yamada, M., Okada, Y., Ishida, Y., Nishihara, H., Tanaka, S., and Nagashima, K. (2001) *Virology* **286,** 100–112
29. Komagome, R., Sawa, H., Suzuki, T., Suzuki, Y., Tanaka, S., Atwood, W. J., and Nagashima, K. (2002) *J. Virol.* **76,** 12992–13000
30. Okada, Y., Sawa, H., Tanaka, S., Takada, A., Suzuki, S., Hasegawa, H., Umemura, T., Fujisawa, J., Tanaka, Y., Hall, W. W., and Nagashima, K. (2000) *J. Biol. Chem.* **275,** 17016–17023
31. Qu, Q., Sawa, H., Suzuki, T., Semba, S., Henmi, C., Okada, Y., Tsuda, M., Tanaka, S., Atwood, W. J., and Nagashima, K. (2004) *J. Biol. Chem.* **279,** 27735–27742
32. Pierre, P., Scheel, J., Rickard, J. E., and Kreis, T. E. (1992) *Cell* **70,** 887–900
33. Takakuwa, H., Goshima, F., Koshizuka, T., Murata, T., Daikoku, T., and Nishiyama, Y. (2001) *Genes Cells* **6,** 955–966
34. Fukata, Y., Itoh, T. J., Kimura, T., Menager, C., Nishimura, T., Shiromizu, T., Watanabe, H., Inagaki, N., Iwamatsu, A., Hotani, H., and Kaibuchi, K. (2002) *Nature Cell Biol.* **4,** 583–591
35. Hergovich, A., Lisztwan, J., Barry, R., Ballschmieter, P., and Krek, W. (2003) *Nature Cell Biol.* **5,** 64–70
36. Higuchi, O., Amano, T., Yang, N., and Mizuno, K. (1997) *Oncogene* **14,** 1819–1825
37. Kuroda, S., Nakagawa, N., Tokunaga, C., Tatematsu, K., and Tanizawa, K. (1999) *J. Cell Biol.* **144,** 403–411
38. Endo, S., Okada, Y., Orba, Y., Nishihara, H., Tanaka, S., Nagashima, K., and Sawa, H. (2003) *J. Neurovirol.* **9,** Suppl. 1, 10–14
39. Dent, E. W., and Gertler, F. B. (2003) *Neuron* **40,** 209–227
40. Clayson, E. T., Brando, L. V., and Compans, R. W. (1989) *J. Virol.* **63,** 2278–2288
41. Gindhart, J. G., Chen, J., Faulkner, M., Gandhi, R., Doerner, K., Wisniewski, T., and Nandlestadt, A. (2003) *Mol. Biol. Cell* **14,** 3356–3365
42. Brady, S. T. (1985) *Nature* **317,** 73–75
43. Vale, R. D., Reese, T. S., and Sheetz, M. P. (1985) *Cell* **42,** 39–50
44. Martin, M., Iyadurai, S. J., Gassman, A., Gindhart, J. G., Jr., Hays, T. S., and Saxton, W. M. (1999) *Mol. Biol. Cell* **10,** 3717–3728
45. Goldstein, L. S. (2001) *Proc. Natl. Acad. Sci. U. S. A.* **98,** 6999–7003
46. Stebbings, H. (2001) *Int. Rev. Cytol.* **211,** 1–31
47. Etienne-Manneville, S., and Hall, A. (2003) *Curr. Opin. Cell Biol.* **15,** 67–72
48. Fukata, M., Nakagawa, M., and Kaibuchi, K. (2003) *Curr. Opin. Cell Biol.* **15,** 590–597
49. Miyoshi, K., Honda, A., Baba, K., Taniguchi, M., Oono, K., Fujita, T., Kuroda, S., Katayama, T., and Tohyama, M. (2003) *Mol. Psychiatry* **8,** 685–694
50. Nakata, T., and Hirokawa, N. (2003) *J. Cell Biol.* **162,** 1045–1055
51. Setou, M., Hayasaka, T., and Yao, I. (2004) *J. Neurobiol.* **58,** 201–206
52. Diefenbach, R. J., Miranda-Saksena, M., Diefenbach, E., Holland, D. J., Boadle, R. A., Armati, P. J., and Cunningham, A. L. (2002) *J. Virol.* **76,** 3282–3291
53. Shinohara, T., Nagashima, K., and Major, E. O. (1997) *Virology* **228,** 269–277

EMBO
reports

scientific report

Dissociation of heterochromatin protein 1 from lamin B receptor induced by human polyomavirus agnoprotein: role in nuclear egress of viral particles

Yuki Okada[1,2,3], Tadaki Suzuki[1,3*], Yuji Sunden[1,2,3], Yasuko Orba[1,3], Shingo Kose[5], Naoko Imamoto[5], Hidehiro Takahashi[6], Shinya Tanaka[1,3], William W. Hall[7], Kazuo Nagashima[1,3] & Hirofumi Sawa[3,4,8+]*

[1]Laboratory of Molecular and Cellular Pathology, and [2]Laboratory of Comparative Pathology, Graduate School of Hokkaido University, Sapporo, Japan, [3]CREST, JST, Sapporo, Japan, [4]21st Century COE Program for Zoonosis Control, Graduate School of Hokkaido University, Sapporo, Japan, [5]Cellular Dynamics Laboratory, RIKEN, Discovery Research Institute, Wako, Saitama, Japan, [6]Department of Pathology, NIHD, Toyama, Shinjuku, Tokyo, Japan, [7]Department of Medical Microbiology, University College, Dublin, Ireland, and [8]Department of Molecular Biology and Diagnosis, Hokkaido University Research Center for Zoonosis Control, Sapporo, Japan

The nuclear envelope is one of the chief obstacles to the translocation of macromolecules that are larger than the diameter of nuclear pores. Heterochromatin protein 1 (HP1) bound to the lamin B receptor (LBR) is thought to contribute to reassembly of the nuclear envelope after cell division. Human polyomavirus agnoprotein (Agno) has been shown to bind to HP1α and to induce its dissociation from LBR, resulting in destabilization of the nuclear envelope. Fluorescence recovery after photobleaching showed that Agno increased the lateral mobility of LBR in the inner nuclear membrane. Biochemical and immunofluorescence analyses showed that Agno is targeted to the nuclear envelope and facilitates the nuclear egress of polyomavirus-like particles. These results indicate that dissociation of HP1α from LBR and consequent perturbation of the nuclear envelope induced by polyomavirus Agno promote the translocation of virions out of the nucleus.

[1]Laboratory of Molecular and Cellular Pathology, and [2]Laboratory of Comparative Pathology, Graduate School of Hokkaido University, N15, W7, Kita-ku, Sapporo 060-8638, Japan
[3]CREST, JST, Sapporo 060-8638, Japan
[4]21st Century COE Program for Zoonosis Control, Graduate School of Hokkaido University, Sapporo 060-8638, Japan
[5]Cellular Dynamics Laboratory, RIKEN, Discovery Research Institute, Wako, Saitama 351-0198, Japan
[6]Department of Pathology, NIHD, Toyama, Shinjuku, Tokyo 162-8640, Japan
[7]Department of Medical Microbiology, University College, Dublin 4, Ireland
[8]Department of Molecular Biology and Diagnosis, Hokkaido University Research Center for Zoonosis Control, Sapporo 060-8638, Japan
*These authors contributed equally to this work
+Corresponding author. Tel/Fax: +81 11 706 7806;
E-mail: h-sawa@patho2.med.hokudai.ac.jp

Received 6 September 2004; revised 21 March 2005; accepted 24 March 2005; published online 29 April 2005

Keywords: agnoprotein; heterochromatin protein 1; JC virus; lamin B receptor

EMBO reports advance online publication 29 April 2005;
doi:10.1038/sj.embor.7400406

INTRODUCTION

The nuclear envelope (NE) consists of an outer nuclear membrane, an inner nuclear membrane (INM), nuclear pore complexes and the peripheral nuclear lamina located adjacent to the INM. Various proteins of chromatin (histones, heterochromatin protein 1 (HP1), barrier-to-autointegration factor), the nuclear lamina (lamins A, B and C) and the INM (emerin, lamina-associated polypeptide 2β, lamin B receptor (LBR); Salina *et al*, 2001) associate with each other during reconstitution and stabilization of the NE. LBR is an integral protein of the INM and binds to HP1 proteins (Ye & Worman, 1996; Ye *et al*, 1997). The NE presents one of the chief obstacles to transport from the nucleus to the cytoplasm of macromolecules, including the virions of most DNA viruses (Pante & Kann, 2002). The β-herpesvirus gene products UL31 and UL34 induce depolymerization of the nuclear lamina to facilitate the nuclear egress of viral capsids (Muranyi *et al*, 2002). However, the mechanisms by which other DNA viruses exit the nucleus remain unclear, including the JC virus (JCV), which is the causative agent of progressive multifocal leukoencephalopathy and belongs to the family of polyomaviruses. The JCV agnoprotein (Agno) comprises 71 amino acids, is localized predominantly in the perinuclear region and the cytoplasm of infected cells (Okada *et al*, 2002) and is related to DNA-damage-induced cell-cycle regulation (Darbinyan *et al*, 2004). The amino-acid sequence of JCV Agno shares ~60% homology with those of agnoproteins of other polyomaviruses; however, the sequence of the amino-terminal portion is ~90%

identical to those of other polyomaviruses, which is suggestive of conservation of function. We show that the N-terminal region of JCV Agno associates with HP1 *in vivo*, resulting in dissociation of HP1 from LBR. This effect alters the NE and thereby facilitates the release of progeny virions from the nucleus into the cytoplasm without nuclear disintegration.

RESULTS

Human JCV Agno binds to HP1

We initially performed a yeast two-hybrid screen with the conserved N-terminal 24 amino acids of JCV Agno as the bait. From a complementary DNA library of human embryonic kidney (HEK) 293 cells, which are permissive for JCV infection (Suzuki *et al*, 2001), six positive clones were isolated and were found to encode the entire sequence of HP1α and the chromo-shadow domain (CSD) of HP1γ (Fig 1A). Interaction between Agno and either Myc-epitope-tagged human HP1α (Fig 1B) or endogenous HP1α (Fig 1C) was also shown in HEK293 cells. We also performed an immunoprecipitation assay to examine whether Agno binds to HP1β and HP1γ *in vivo*, and found that Agno did not interact with HP1β and HP1γ (Fig 1D), although the CSD of HP1γ was identified by a yeast two-hybrid screening.

Agno interacts with HP1α at the NE

We have reported that the Agno is mainly expressed in the cytoplasm of infected cells (Okada *et al*, 2001), whereas HP1α is expressed in the nucleus. To examine where Agno and HP1α become associated, a mutant of Agno lacking most of the N-terminal HP1α-binding motif, designated C18, was constructed. Subcellular localizations of wild-type (WT) and a C18 mutant of Agno were predominantly observed in the cytoplasm (Fig 2A). Immunoprecipitation analysis showed that C18 did not interact with HP1α, whereas WT Agno bound to HP1α (Fig 2B). The C18 showed cytoplasmic distribution that was similar to WT; however, the C18 did not colocalize with lamin A/C at the NE (Fig 2C). These results indicated that the interaction between Agno and HP1α occurs at the NE.

Agno disrupts the interaction between HP1α and LBR

Some HP1 proteins may be partially localized in the perinuclear region and this may be because of LBR binding (Minc *et al*, 1999). Our yeast two-hybrid analysis indicated that Agno interacts with the CSD of HP1, which is also responsible for the association of these proteins with LBR (Ye *et al*, 1997). These observations led us

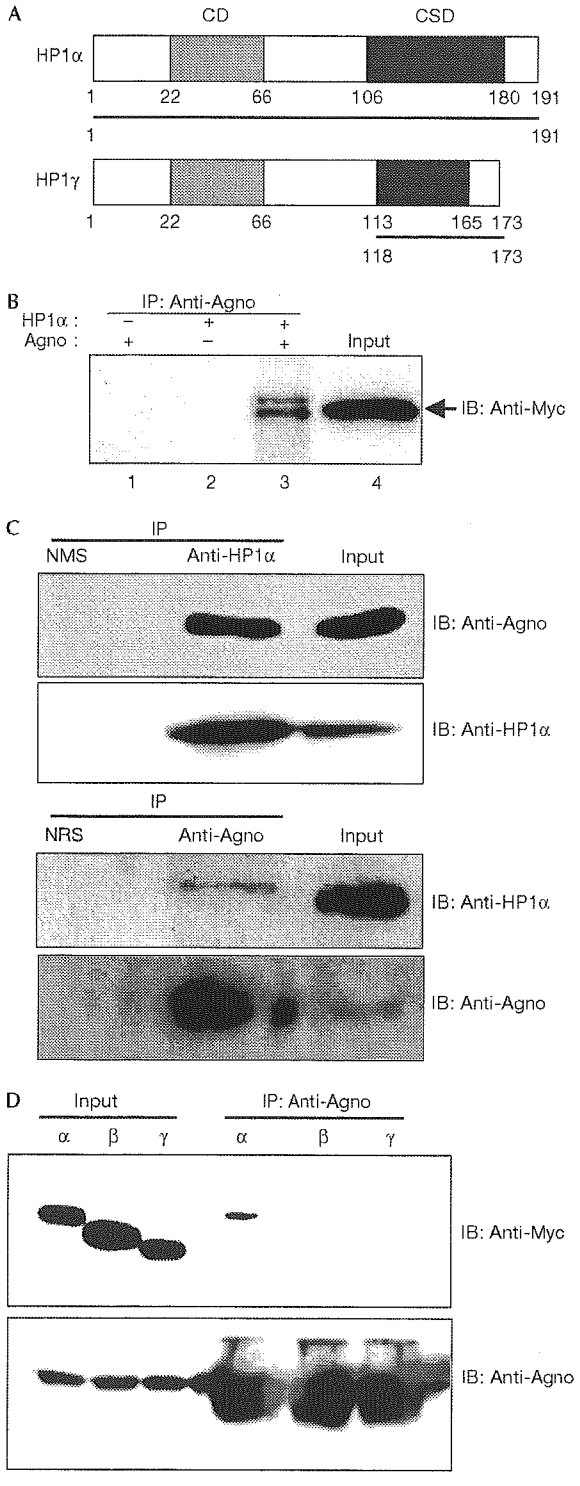

Fig 1 | Interaction of JCV Agno with HP1 *in vivo*. (A) Schematic representation of human HP1α and HP1γ showing the regions (bars) encoded by cDNA fragments isolated by a yeast two-hybrid assay with the N-terminal region of Agno as a bait. CD and CSD, chromo and chromo-shadow domains, respectively. (B) 293AG cells (HEK293 cells in which the expression of JCV Agno is inducible by Dox) were transfected with a vector for Myc-tagged human HP1α and were incubated in the absence or presence of Dox for 24 h. Cell lysates were subjected to immunoprecipitation with antibodies to Agno (anti-Agno), and the resulting precipitates were subjected to immunoblotting (IB) with anti-Myc. (C) Lysates prepared from 293AG cells after treatment with Dox for 48 h were subjected to immunoprecipitation with anti-HP1α or anti-Agno, and the resulting precipitates and cell lysates (Input) were subjected to immunoblotting with the same antibodies, as indicated. NMS, normal mouse serum; NRS, normal rabbit serum. (D) 293T cells were transfected with a vector for Agno and Myc-tagged human HP1α, β or γ, and were subjected to immunoprecipitation with anti-Agno. The resulting precipitates were subjected to immunoblotting with anti-Myc and anti-Agno.

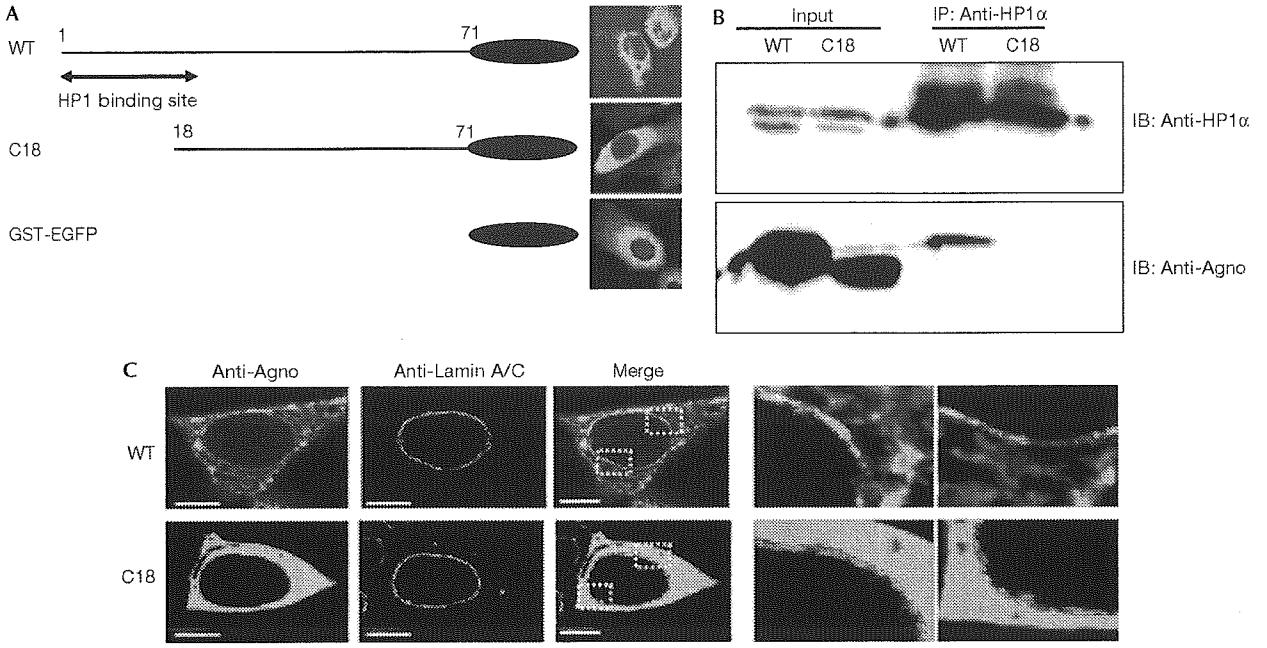

Fig 2 | Impaired ability of an Agno mutant to colocalize or interact with HP1. (A) Schematic representation of GST–EGFP fusion constructs of wild-type (WT) and mutant (C18) forms of Agno and EGFP fluorescence images showing their subcellular localizations in transfected HEK293 cells. (B) Lysates of 293T cells transiently expressing the WT or C18 forms of Agno were subjected to immunoprecipitation (IP) with anti-HP1α, and the resulting precipitates were subjected to immunoblotting (IB) with anti-Agno or anti-HP1α. (C) Immunofluorescence analysis of the expression of GST–EGFP-fused WT or C18 forms of Agno and of endogenous Lamin A/C in HEK293 cells. Enlarged dotted rectangles of the merged images are represented. Scale bars, 5 μm.

to propose that Agno might interfere with the interaction between HP1 and LBR and thereby alter the structure of the NE.

To examine this possibility, we established a cell line, designated 293AG, that is derived from HEK293 cells and in which the expression of JCV Agno subcloned into pcDNA4/TO/Myc–His is under the control of a tetracycline-responsive promoter. All 293AG cells expressed the recombinant Agno (~14 kDa) in 3 h of exposure to doxycycline (Dox), and the level of expression increased gradually with time (Fig 3A). In the absence of Dox, Agno was not detected by immunoblot or immunofluorescence analysis.

We next transfected 293AG cells with a vector for Myc-epitope-tagged HP1α (pCMV–MycHP1α) and subjected lysates prepared from Dox-treated or untreated cells to immunoprecipitation with antibodies to Agno. Immunoblot analysis with antibodies to Myc of precipitates prepared from the Dox-treated cells, but not of those from the untreated cells, showed the presence of HP1α (Fig 3B). We then transfected 293AG cells with both pCMV–MycHP1α and pLBR–EGFP (enhanced green fluorescent protein), and induced Agno expression with Dox treatment. The amount of HP1α that co-precipitated with Agno in these cells was directly related to the level of Agno expression (Fig 3B). Conversely, the amount of HP1α that co-precipitated with LBR–EGFP was inversely related to the level of Agno expression.

Agno increases the lateral mobility of LBR in the NE

Immunofluorescence analysis also showed that Agno colocalized with LBR–EGFP at the NE, and this colocalization was pronounced in invaginated regions of the NE (Fig 4A). The dissociation of LBR from heterochromatin results in structural changes in the NE, including the formation of invaginations and protrusions (Mazlo *et al*, 2001); such changes are also characteristic of JCV-infected oligodendrocytes in the brains of patients with progressive multifocal leukoencephalopathy.

Disruption of the interaction between HP1 and LBR by Agno might be expected to increase the lateral mobility of LBR in the NE. We examined this possibility by fluorescence recovery after photobleaching (FRAP) analysis in 293AG cells stably expressing LBR–EGFP. Photobleaching was induced at the nuclear rim, and recovery of fluorescence was monitored with a series of low-intensity scans. LBR–EGFP fluorescence in the bleached region of the nuclear rim recovered faster in cells expressing Agno than in those not exposed to Dox (Fig 4B,C); the mean recovery ratio at 10 min after photobleaching was significantly higher in the presence of Agno (Fig 4D). We also subjected the EGFP-fused full-length LBR (Haraguchi *et al*, 2000) to the FRAP analyses, and obtained results similar to those using the LBR–EGFP (data not shown). These observations indicated that Agno-induced dissociation of the LBR–HP1 complex resulted in an increase in the lateral mobility of LBR in the INM.

Agno facilitates nuclear egress of progeny virions

We proposed that the alteration of the NE induced by Agno might facilitate the nuclear release of progeny virions. To examine this possibility, we microinjected virus-like particles (VLPs) consisting of recombinant JCV VP1 into the nuclei of 293AG cells with or

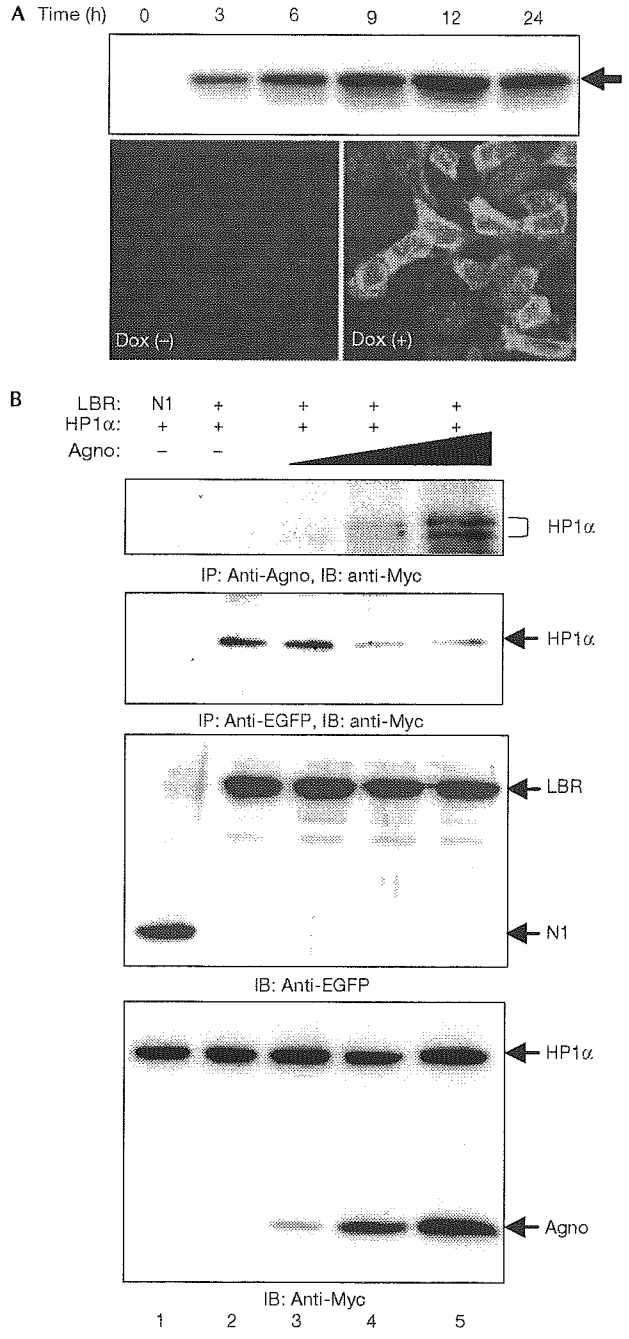

Fig 3 | Agno-induced dissociation of the HP1α–LBR complex *in vivo*. (**A**) 293AG cells were incubated with Dox for the indicated times, after which cell lysates were subjected to immunoblotting with anti-Agno. Cells incubated with or without Dox for 24 h were also subjected to immunofluorescence analysis with anti-Agno. (**B**) 293AG cells were transfected with pEGFP-N1 or pLBR–EGFP together with pCMV–MycHP1α. The transfected cells were treated with Dox for 0, 3, 7 or 24 h. Cell lysates were then subjected to immunoprecipitation (IP) with anti-Agno or anti-EGFP, and the resulting precipitates were subjected to immunoblotting (IB) with anti-Myc. Cell lysates were also subjected directly to immunoblotting with anti-EGFP or anti-Myc.

without Dox treatment. Such VLPs manifest a virion-like structure and physiological functions, including cellular attachment, intracytoplasmic transport and nuclear entry (Goldmann *et al*, 1999; Suzuki *et al*, 2001; Komagome *et al*, 2002; Qu *et al*, 2004), similar to those of JCV virions. We used Cy3 as a nuclear injection marker, which usually remained at the injection site. In the absence of Agno expression, most of the VLPs injected into the nucleus remained there 1 h later (Fig 5). In contrast, VLP fluorescence was not detected at this time in the nucleus of cells expressing Agno, suggesting that Agno promoted translocation of VLPs from the nucleus to the cytoplasm. Simultaneously, a certain amount of Cy3 also leaked into the cytoplasm in Dox (+) cells; however, it remained in the nucleus without Dox treatment. These observations indicate that the alteration of NE by Agno might facilitate nuclear egress of the progeny virions, and considering the behaviour of Cy3, this effect was not specific to virus particles.

DISCUSSION

The INM is linked to lamina and chromatin through interactions of its integral membrane proteins, including LBR. In the late stage of JCV infection, the nuclei of infected cells are filled with progeny virions and show structural alterations of the NE, such as invaginations and protrusions (Mazlo *et al*, 2001). We have shown that JCV Agno competes with LBR for binding to HP1, resulting in destabilization of the NE. Although viral protein-induced destabilization of the NE and a role for LBR have previously been described in herpesvirus infection (Scott & O'Hare, 2001; Muranyi *et al*, 2002), the role of LBR in this instance might be an indirect consequence of the depolymerization of lamin A/C that results from the virus-induced recruitment of protein kinase C to the INM. The association between LBR and its main ligand lamin B is also preserved during herpesvirus infection. LBR binds to a range of proteins (Ye & Worman, 1994, 1996), of which chromatin and chromatin-related proteins are thought to function as nucleoplasmic ligands that immobilize LBR in the INM (Ellenberg *et al*, 1997). LBR thus has a key role in the association of HP1 with the NE. Our data show that JCV Agno induces dissociation of HP1 from LBR by competitive binding to HP1, which caused an increase in the lateral mobility of LBR. This is the first evidence, to our knowledge, of a viral-protein-induced alteration of the NE through dissociation of HP1 and LBR.

In addition, expression of Agno also facilitated the nuclear export of VLPs without inducing nucleolysis, which is thought to mimic the nuclear egress of progeny virions in virus-infected cells. Consistent with this notion, agnogene-deficient simian virus 40 (SV40) shows a reduced capacity for cell-to-cell spread (Resnick & Shenk, 1986). Furthermore, we recently showed by RNA interference that JCV Agno is required for viral propagation (Orba *et al*, 2004). Together, our observations suggest that Agno facilitates viral propagation by promoting viral spreading. This function of JCV Agno is probably shared by agnoproteins of SV40 and human polyomavirus BK (BKV), given that the N-terminal region of JCV Agno is highly homologous to those of the SV40 and BKV proteins and is responsible for binding to HP1α.

METHODS

Plasmid construction. A cDNA encoding the first 238 amino acids of LBR was amplified by PCR from an HEK293 cell

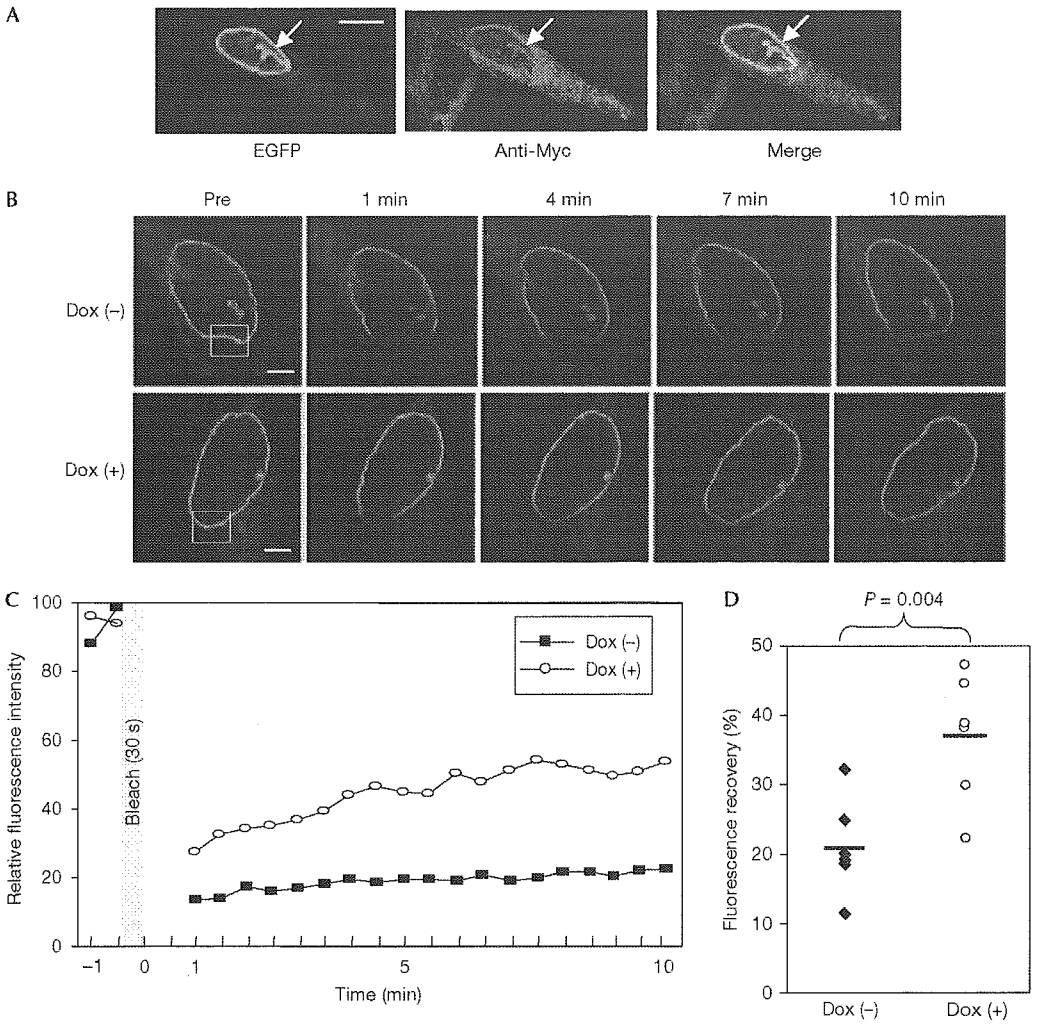

Fig 4 | Agno-induced increase in the lateral mobility of LBR. (**A**) Colocalization of LBR–EGFP detected by EGFP fluorescence and Agno detected with anti-Myc in 293AG cells. Arrows indicate an invagination of the NE in which LBR–EGFP and Agno are colocalized. Scale bar, 10 μm. (**B**) FRAP analysis of 293AG cells expressing LBR–EGFP and incubated in the absence or presence of Dox for 24 h. The fluorescence of LBR–EGFP in the boxed regions of the nuclear rim was irreversibly photobleached, and the recovery of fluorescence in these regions was monitored for 10 min. Representative images before (Pre) and at 1, 4, 7 and 10 min after bleaching are shown. Scale bars, 2 μm. (**C**) Quantification of the fluorescence recovery shown in (**B**). (**D**) Summary of fluorescence recovery ratios at 10 min after photobleaching. Each point represents an individual cell and the horizontal bars indicate the median values. The statistical significance of the difference between the two mean values was calculated by Student's two-tailed *t*-test.

cDNA library and subcloned into pEGFP-N1 (BD Biosciences Clontech, Franklin Lakes, NJ, USA), yielding pLBR–EGFP (Gerlich *et al*, 2001; Beaudouin *et al*, 2002). In addition, the pEGFP vector containing the full-length LBR, designated as hLBR in pEGFP-N3, was provided by Dr Haraguchi (Haraguchi *et al*, 2000). A full-length HP1α cDNA was also amplified from the HEK293 cell cDNA library and was subcloned into pCMV–Myc (Clontech). For expression of JCV Agno, the cDNA was subcloned into either pGST–EGFP.pcDNA4HisMax (GST: glutathione-*S*-transferase) or pcDNA4/TO/Myc–His (Invitrogen, Carlsbad, CA, USA).

FRAP analysis. We performed the FRAP analysis according to Ellenberg *et al* (1997) and Scott & O'Hare (2001), with several technical modifications, because the performance of our laser scanning microscope (LSM) system was different from the LSM systems that they used. As the laser intensity of our LSM system was much lower than their system, our bleaching time was longer than their experiments. FRAP analysis of 293AG cells stably expressing LBR–EGFP was performed with the Olympus FV300 confocal microscope fitted with a ×60 oil-immersion objective (numerical aperture, 1.25). The cells (2×10^5) were plated on 35-mm dishes coated with type I collagen and were incubated with or without Dox for 24 h before analysis. Images were recorded at 488 nm (at 3% power) and an intense pulse of laser light (100% power) was then applied for 30 s to bleach the fluorescent molecules in a defined region (2 × 2 μm). Recovery of fluorescence was monitored at 30 s intervals for 10 min by scanning with attenuated laser light (3% power). The FV300

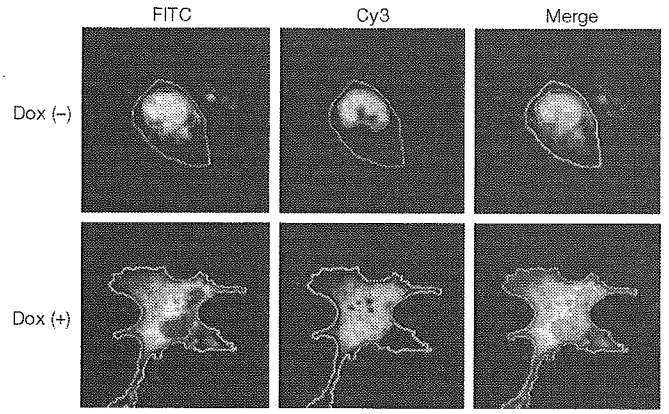

Fig 5 | Agno facilitates the nuclear egress of VLPs. The nuclei of Dox-treated (lower panels) or untreated (upper panels) 293AG cells were microinjected with VLPs and Cy3 (injection site marker; red fluorescence), and, after 1 h, the cells were subjected to immunofluorescence analysis with anti-VP1 (green). Blue lines indicate the rim of the nuclei and white lines indicate the edge of the cytoplasm.

software was used to generate a time series from the images and to plot the pixel intensity in the defined regions of interest for the duration of the experiment. At each time point, the intensity of an equivalent background area was subtracted and values were normalized for total loss of fluorescence. The relative recovery of fluorescence intensity was calculated as 100% × ((intensity at the recovery plateau)−(intensity at 1 min after bleaching))/((average intensity of the bleached region before bleaching)−(intensity at 1 min after bleaching)). We also subjected the pEGFP vector containing the full-length LBR (provided by Dr Haraguchi) to the FRAP analyses (Haraguchi *et al*, 2000).

Supplementary information is available at *EMBO reports* online (http://www.emboreports.org).

ACKNOWLEDGEMENTS

We thank M. Satoh and M. Sasada for technical assistance; A. Kihara, M. Matsuda and N. Mochizuki for helpful suggestions; and T. Haraguchi for the hLBR in pEGFP-N3 plasmid. Y.O. is a Research Fellow of the Japan Society for the Promotion of Science. This study was supported in part by grants from the Ministry of Education, Science, Technology, Sports, and Culture of Japan, The Ministry of Health, Labor, and Welfare of Japan, The Japan Human Science Foundation.

REFERENCES

Beaudouin J, Gerlich D, Daigle N, Eils R, Ellenberg J (2002) Nuclear envelope breakdown proceeds by microtubule-induced tearing of the lamina. *Cell* **108:** 83–96

Darbinyan A, Siddiqui KM, Slonina D, Darbinian N, Amini S, White MK, Khalili K (2004) Role of JC virus agnoprotein in DNA repair. *J Virol* **78:** 8593–8600

Ellenberg J, Siggia ED, Moreira JE, Smith CL, Presley JF, Worman HJ, Lippincott-Schwartz J (1997) Nuclear membrane dynamics and reassembly in living cells: targeting of an inner nuclear membrane protein in interphase and mitosis. *J Cell Biol* **138:** 1193–1206

Gerlich D, Beaudouin J, Gebhard M, Ellenberg J, Eils R (2001) Four-dimensional imaging and quantitative reconstruction to analyse complex spatiotemporal processes in live cells. *Nat Cell Biol* **3:** 852–855

Goldmann C *et al* (1999) Molecular cloning and expression of major structural protein VP1 of the human polyomavirus JC virus: formation of virus-like particles useful for immunological and therapeutic studies. *J Virol* **73:** 4465–4469

Haraguchi T, Koujin T, Hayakawa T, Kaneda T, Tsutsumi C, Imamoto N, Akazawa C, Sukegawa J, Yoneda Y, Hiraoka Y (2000) Live fluorescence imaging reveals early recruitment of emerin, LBR, RanBP2, and Nup153 to reforming functional nuclear envelopes. *J Cell Sci* **113:** 779–794

Komagome R, Sawa H, Suzuki T, Suzuki Y, Tanaka S, Atwood WJ, Nagashima K (2002) Oligosaccharides as receptors for JC virus. *J Virol* **76:** 12992–13000

Mazlo M, Ressetar HG, Stoner GL (2001) The neuropathology and pathogenesis of progressive multifocal leukoencephalopathy. *Hum Polyomaviruses: Mol and Clin Perspect* 257–335

Minc E, Allory Y, Worman HJ, Courvalin JC, Buendia B (1999) Localization and phosphorylation of HP1 proteins during the cell cycle in mammalian cells. *Chromosoma* **108:** 220–234

Muranyi W, Haas J, Wagner M, Krohne G, Koszinowski UH (2002) Cytomegalovirus recruitment of cellular kinases to dissolve the nuclear lamina. *Science* **297:** 854–857

Okada Y, Endo S, Takahashi H, Sawa H, Umemura T, Nagashima K (2001) Distribution and function of JCV agnoprotein. *J Neurovirol* **7:** 302–306

Okada Y, Sawa H, Endo S, Orba Y, Umemura T, Nishihara H, Stan AC, Tanaka S, Takahashi H, Nagashima K (2002) Expression of JC virus agnoprotein in progressive multifocal leukoencephalopathy brain. *Acta Neuropathol (Berl)* **104:** 130–136

Orba Y, Sawa H, Iwata H, Tanaka S, Nagashima K (2004) Inhibition of virus production in JC virus-infected cells by postinfection RNA interference. *J Virol* **78:** 7270–7273

Pante N, Kann M (2002) Nuclear pore complex is able to transport macromolecules with diameters of about 39 nm. *Mol Biol Cell* **13:** 425–434

Qu Q, Sawa H, Suzuki T, Semba S, Henmi C, Okada Y, Tsuda M, Tanaka S, Atwood WJ, Nagashima K (2004) Nuclear entry mechanism of the human polyomavirus JC virus-like particle: role of importins and the nuclear pore complex. *J Biol Chem* **279:** 27735–27742

Resnick J, Shenk T (1986) Simian virus 40 agnoprotein facilitates normal nuclear location of the major capsid polypeptide and cell-to-cell spread of virus. *J Virol* **60:** 1098–1106

Salina D, Bodoor K, Enarson P, Raharjo WH, Burke B (2001) Nuclear envelope dynamics. *Biochem Cell Biol* **79:** 533–542

Scott ES, O'Hare P (2001) Fate of the inner nuclear membrane protein lamin B receptor and nuclear lamins in herpes simplex virus type 1 infection. *J Virol* **75:** 8818–8830

Suzuki S, Sawa H, Komagome R, Orba Y, Yamada M, Okada Y, Ishida Y, Nishihara H, Tanaka S, Nagashima K (2001) Broad distribution of the JC virus receptor contrasts with a marked cellular restriction of virus replication. *Virology* **286:** 100–112

Ye Q, Worman HJ (1994) Primary structure analysis and lamin B and DNA binding of human LBR, an integral protein of the nuclear envelope inner membrane. *J Biol Chem* **269:** 11306–11311

Ye Q, Worman HJ (1996) Interaction between an integral protein of the nuclear envelope inner membrane and human chromodomain proteins homologous to *Drosophila* HP1. *J Biol Chem* **271:** 14653–14656

Ye Q, Callebaut I, Pezhman A, Courvalin JC, Worman HJ (1997) Domain-specific interactions of human HP1-type chromodomain proteins and inner nuclear membrane protein LBR. *J Biol Chem* **272:** 14983–14989

Transcriptional co-activator activity of SYT is negatively regulated by BRM and Brg1

Michiko Ishida[1], Shinya Tanaka[2], Misao Ohki[1] and Tsutomu Ohta[1,*]

[1]*Center for Medical Genomics, National Cancer Center Research Institute, 5-1-1 Tsukiji Chuo-ku, Tokyo 104-0045, Japan*
[2]*Laboratory of Molecular and Cellular Pathology, Hokkaido University School of Medicine, N15, W7, Kita-ku, Sapporo 060-8638, Japan*

The t(X;18)(p11.2;q11.2) translocation found in synovial sarcomas results in the fusion of the SYT gene on chromosome 18 to the SSX gene on chromosome X. Although the SYT-SSX fusion proteins may trigger synovial sarcoma development, the biological functions of SYT, SSX and SYT-SSX genes are unclear. Transfections of Gal4 DNA binding domain fusion protein constructs demonstrate that SYT protein acts as a transcriptional co-activator at the C-terminal domain and that the activity is repressed through the N-terminus. The N-terminal 70 amino acids of SYT bind not only to BRM, but also to Brg1, both of which are subunits of SWI/SNF chromatin remodelling complexes. Here, we have investigated the functions of BRM and Brg1 on the repression of SYT activity. The negative regulation of SYT transcriptional co-activator activity is dependent on the ATP-hydrolysis of BRM and Brg1 in the protein complexes. This indicates that the SWI/SNF protein complexes regulate SYT activity using the chromatin remodelling activity.

Introduction

Synovial sarcoma is a soft tissue tumour and mainly appears in young adults limbs (dos Santos *et al.* 2001). Cytogenetical analysis indicates that chromosomal translocation, t(X;18)(p11.2;q11.2) causes the majority of these tumours (Turc-Carel *et al.* 1987). The molecular analysis of the breakpoints has shown that the SYT (synovial sarcoma translocation) gene on chromosome 18q11.2 is disrupted and juxtaposed to SSX (synovial sarcoma X chromosome breakpoint) genes on Xp11.2 in a mutually exclusive fashion. The fusion gene is transcribed and translated as a chimeric SYT-SSX protein (Clark *et al.* 1994). The normal SYT gene is expressed in wide range of human tissues and cell lines, including those derived from synovial sarcoma (Crew *et al.* 1995). The protein has two functional domains; a conserved 54-amino acid N-terminal domain and a C-terminal domain rich in glycine, proline, glutamine and tyrosine (QPGY domain) that functions as a transcriptional activator (Thaete *et al.* 1999). The SYT lacks obvious DNA binding domains, therefore the biological function of SYT is still unclear. The SSX genes are part of a family of which six members have been identified on the X chromosome (dos Santos *et al.* 2001). They have restricted expression in normal tissues, confined to the testis and lower levels in the thyroid (Gure *et al.* 1997). SSX proteins contain a KRAB (Kruppel-associated box) domain at the N-terminus and an SSXRD (SSX repression domain) at the C-terminus (Lim *et al.* 1998). The SYT-SSX1 fusion gene is translated into a chimeric protein in which the C-terminal 8 amino acids of the SYT protein are replaced by 78 amino acids (amino acid residues 111–188) from the SSX1 C-terminus (Clark *et al.* 1994; dos Santos *et al.* 2001). Although the SYT-SSX fusion proteins may trigger synovial sarcoma development, the biological functions of SYT, SSX and SYT-SSX genes are unclear.

It was shown that SYT interacts and co-localizes with BRM (Thaete *et al.* 1999), which is one of components of human SWI/SNF complexes (Wang *et al.* 1996; Kornberg & Lorch 1999; Vignali *et al.* 2000). The SWI/SNF complex was first characterized in *Saccharomyces cerevisiae* and affected transcriptional activity by modifying the chromatin structure in vicinity of target promoters (Vignali *et al.* 2000). As the activity of yeast SWI/SNF complex is dependent on an ATP-hydrolysis, SWI2 protein, which is a subunit of the complex and has a DNA-dependent ATPase activity, is a key player. Two proteins, BRM and Brg1, closely related to the yeast SWI2 have been identified in humans. These proteins are associated with human SWI/SNF complex, composed of at least eight other proteins, including

Communicated by: Masayuki M. Yamamoto
**Correspondence*: Email: cota@gan2.res.ncc.go.jp

DOI: 10.1111/j.1356-9597.2004.00737.x

a yeast SNF5 homologue BAF47b. Within this complex, the two SWI2-related proteins are mutually exclusive, indicating at least two versions of the human SWI/SNF complexes. Both BRM and Brg1 can interact with BAF47b, indicating that the two proteins have common molecular partners of BAF47b (Muchardt *et al.* 1995). It was known that the human SWI/SNF complexes can positively and negatively regulate gene expressions.

Although it was shown that the SYT is a transcriptional co-activator and interacts with BRM (Thaete *et al.* 1999), there is no evidence demonstrating the functional effects of BRM on SYT activity. In this paper, we report that BRM and its homologue, Brg1, repress the transactivation of SYT. The repression by BRM or Brg1 correlates with its ATP-hydrolysis activity as a functional component of the human SWI/SNF complex. Interestingly, this repression is independent of HDAC activity.

Results

N-terminal domain negatively regulates the transcriptional activity of C-terminal domain in SYT

The human SYT protein is composed of 387 amino acids and has no homology to any known protein. The protein has a C-terminal domain, rich in glycine, proline, glutamine and tyrosine (QPGY domain), that is found in several transcriptional activators. It was shown that SYT is a transcriptional co-activator (Brett *et al.* 1997; Thaete *et al.* 1999). Because the SYT lacks obvious DNA binding domains, to find the SYT functional domain in the transactivation, we analysed a luciferase reporter assay by fusing SYT and its deletion mutants to the Gal4 DNA binding domain (Fig. 1A). The transcriptional activity of the C-terminal domain (SYT-E) was strong, but that of the wild-type (SYT-WT) or the N-terminal domain (SYT-A) was weak, in the 293T cell (Fig. 1B). This result suggests that the N-terminal domain negatively regulates the transcriptional activity of the C-terminal domain in SYT, the same as previously reported (Brett *et al.* 1997).

BRM and Brg1 interact and co-localize with SYT

Recently, it was shown that a chicken BRM binds to SYT *in vitro* (Thaete *et al.* 1999) and that human BRM (amino acid residues 156–205) interacts with SYT N-terminal domain by co-immunoprecipitation analysis (Nagai *et al.* 2001). BRM is one of components of the SWI/SNF complex, which is involved in chromatin structure remodelling in an ATP-hydrolysis-dependent fashion (Vignali *et al.* 2000). We found that the interaction domain of BRM with SYT shares homology with Brg1 (Fig. 2A), which is another component of SWI/SNF complexes. To examine the direct interaction between SYT and BRM or Brg1, we analysed a binding activity of the full length of BRM or Brg1 to the SYT N-terminal domain. Gal4-SYT mutants that contain SYT-A (amino acid residues 1–180), SYT-B (amino acid residues 1–70) and SYT-C (amino acid residues 71–180) were fused to GST (glutathione S-transferase) protein. GST-Gal4-SYT mutant proteins purified from *Escherichia coli* were immobilized on glutathione-sepharose beads and incubated with full-length BRM or Brg1 purified from Sf9 cells. After washing the beads, the bound proteins were separated by SDS–PAGE and detected by anti-BRM and anti-Brg1 antibodies, respectively. BRM and Brg1 interacted with GST-SYT-A and GST-SYT-B, but not GST-SYT-C (Fig. 2B, lanes 7, 8 and 9, and Fig. 2C, lanes 7, 8 and 9). These results suggest that both BRM and Brg1 bind to the N-terminal 70 amino acids of SYT.

To examine whether BRM and Brg1 are able to bind to full-length SYT in mammalian cells, we performed an immunoprecipitation assay with the 293T cell. When flag-tagged SYT-WT expression vector was co-transfected with BRM or Brg1, BRM or Brg1 was co-immunoprecipitated with SYT by anti-flag antibody M2 (Fig. 2D, lanes 3 and 7). However, when flag-tagged SYT-D that was deleted N-terminal domain was used, BRM or Brg1 was not co-immunoprecipitated (Fig. 2D, lanes 4 and 8). These results suggested that BRM and Brg1 interact with SYT through its N-terminal 70 amino acids in the cell.

For a further validation of the SYT/BRM and SYT/Brg1 interactions, we determined the subcellular localizations of these proteins using immunofluorescence assay. A full-length SYT was cloned in-frame with the green fluorescent protein (GFP) construct. GFP-SYT was co-transfected with BRM or Brg1 in the SW13 cell. After co-transfection, GFP-SYT was detected by autofluorescence. BRM and Brg1 were detected by specific antibodies, respectively. GFP-SYT green signals and Brg1 red signals were observed in punctate configurations (Fig. 2E, a and b). After overlay, a mixed colour (yellow) was observed for almost every signal (Fig. 2E,c), which is indicative of a co-localization of SYT and Brg1. DAPI counter-staining (Fig. 2E,d) indicated that the co-localizing signals were present in the nucleus. Similar co-localization of SYT and BRM in the nucleus was observed (Fig. 2E,e–h). A punctate pattern of co-localization signals was also observed after transfection with flag-tagged full-length SYT and Brg1 (data not shown).

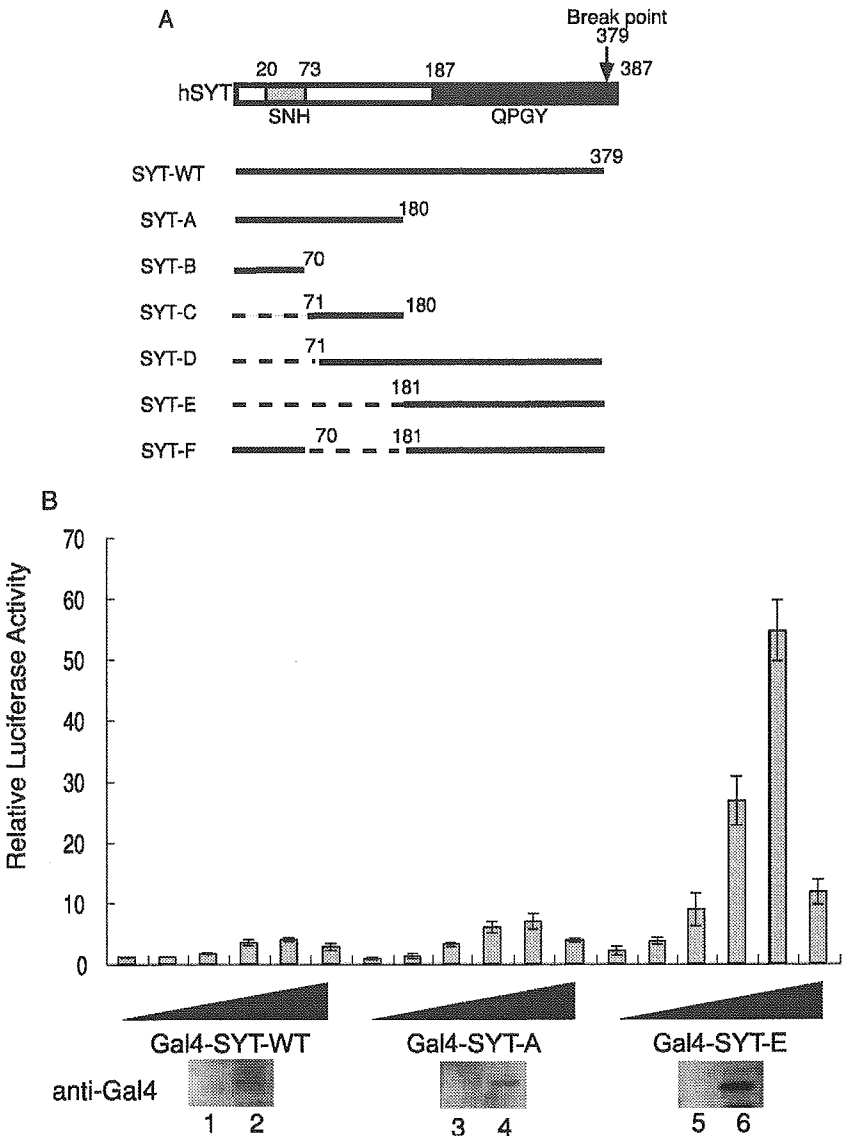

Figure 1 Schematic structures and transcriptional co-activator activities of SYT and its deletion mutant proteins. (A) All constructs have fused to the Gal4 DNA binding domain (Gal4). Numbers indicate the amino acid positions. The arrow represents the position of translocation to SSXs in synovial sarcoma. The SYT protein has two functional domains; a conserved 54-amino acid N-terminal domain and a C-terminal domain rich in glycine, proline, glutamine and tyrosine (QPGY domain). (B) Transcriptional activities of Gal4-SYT proteins in the 293T cell. pG5luc reporter (0.25 μg) was co-transfected with increasing amounts (0.1 ng, 0.5 ng, 2 ng, 10 ng, 0.1 μg and 0.5 μg) of Gal4-SYT-WT, Gal4-SYT-A and Gal4-SYT-E in the 293T cell. Luciferase activity in the cell lysate was normalized with *Renilla* luciferase activity of pTK-RL as an internal control. The activity in the presence of pG5luc and pGal4-DBD (Gal4 DNA binding domain alone) was set at 1. The amounts of expressed products of 0.1 and 0.5 μg of Gal4-SYT-WT (lanes 1 and 2), Gal4-SYT-A (lanes 3 and 4) and Gal4-SYT-E (lanes 5 and 6) were detected by anti-Gal4DBD antibody.

BRM and Brg1 negatively regulate transcriptional activity of SYT

To examine whether BRM or Brg1 has any effects on the SYT transcriptional activity, we analysed the activities of SYT-WT, SYT-A and SYT-E in the SW13 cell that expresses undetectable levels of BRM and Brg1 (Wang *et al.* 1996; DeCristofaro *et al.* 2001). SYT-WT showed strong transcriptional activity similar to SYT-E in both the BRM- and Brg1-deficient cell lines (Fig. 3A). This result suggests that the N-terminal domain (amino acids 1–180) of SYT has no effect on the transcriptional co-activator activity of its C-terminal domain (amino acids 181–379) in the BRM- and Brg1-deficient cells, unlikely in the 293T cell (Fig. 1B). To examine whether the difference of the SYT-WT transcription activity between the SW13 cell and the 293T cell was dependent on expression levels of BRM and Brg1, the SYT-WT activity was analysed by co-transfection of BRM or Brg1 in SW13 and 293T cells. The SYT-WT transcriptional activity was repressed by addition of BRM or Brg1, with dose dependency in the SW13 cell, but not the 293T cell (Fig. 3B,C, and data not shown). In another cell C33A that also expresses undetectable levels of BRM and Brg1 (Wang *et al.* 1996; DeCristofaro *et al.* 2001), the same as the SW13 cell, the SYT-WT activity was repressed by addition of BRM or Brg1 (data not shown). These results suggest that BRM or Brg1 negatively

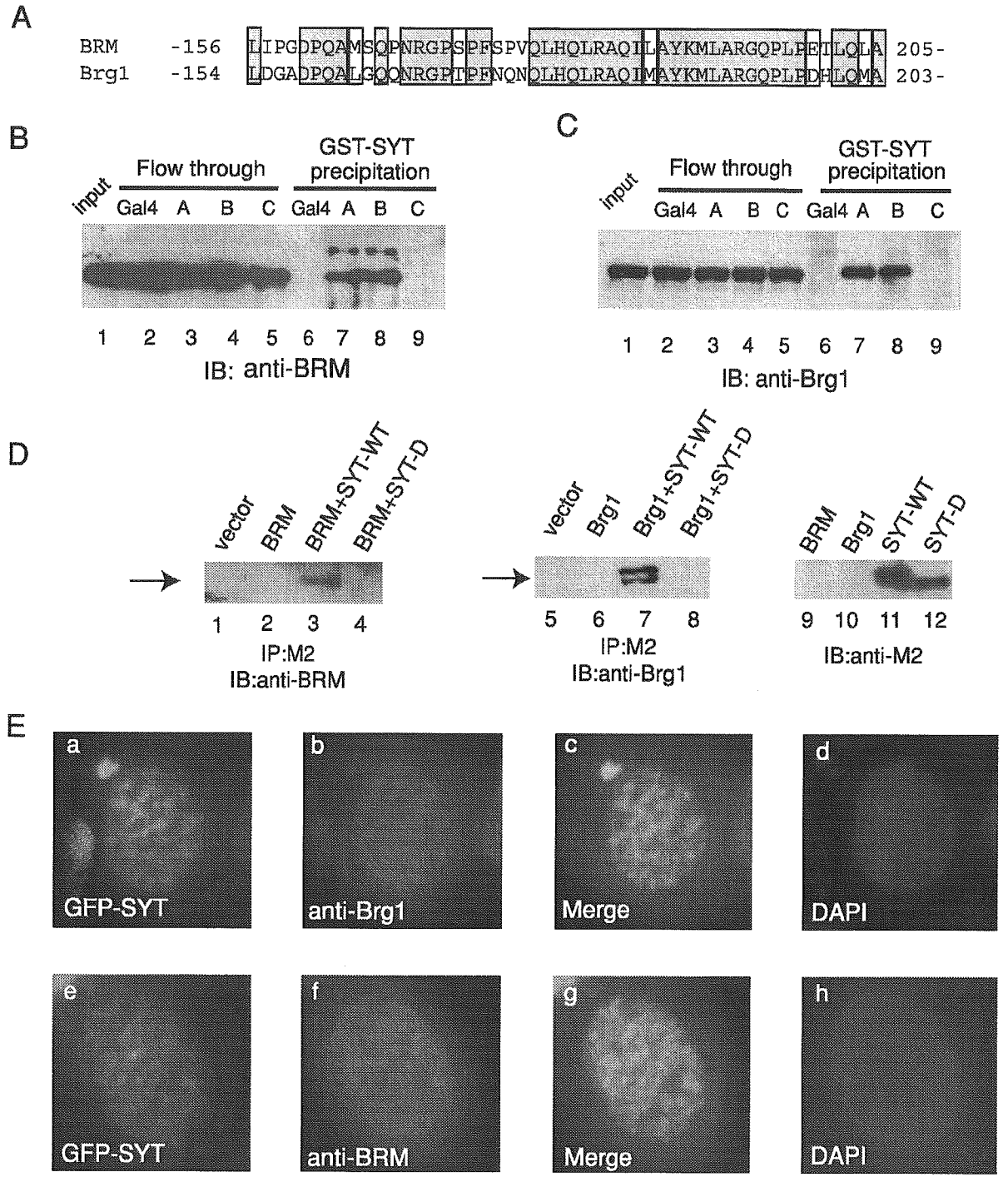

Figure 2 Interactions of the N-terminal 70 amino acids of SYT with BRM and Brg1. (A) Comparison between the region of BRM bound to SYT (Nagai *et al.* 2001) and the homology domain of Brg1. The boxes highlight the amino acids that exhibit identity (shaded) or homology (open). (B, C) Beads bound to GST-Gal4, GST-Gal4-SYT-A (amino acid residues 1–180), GST-Gal4-SYT-B (amino acid residues 1–70) or GST-Gal4-SYT-C (amino acid residues 71–180) were incubated with purified BRM or Brg1. The bound proteins were separated by SDS–PAGE and detected by anti-BRM (B) or anti-Brg1(C) antibody. Lane 1 indicates the input-purified BRM or Brg1 protein. Lanes 2–5 indicate fractions unbound to GST-fusion proteins. Lanes 6–9 indicate fractions bound to GST-fusion proteins. (D) SYT-WT was bound to BRM and Brg1 though its N-terminal domain in cultured cell. Flag-tagged full-length SYT (SYT-WT) or its N-terminal deletion mutant (SYT-D) was co-transfected with BRM or Brg1 into the 293T cell. Flag-tagged SYT was

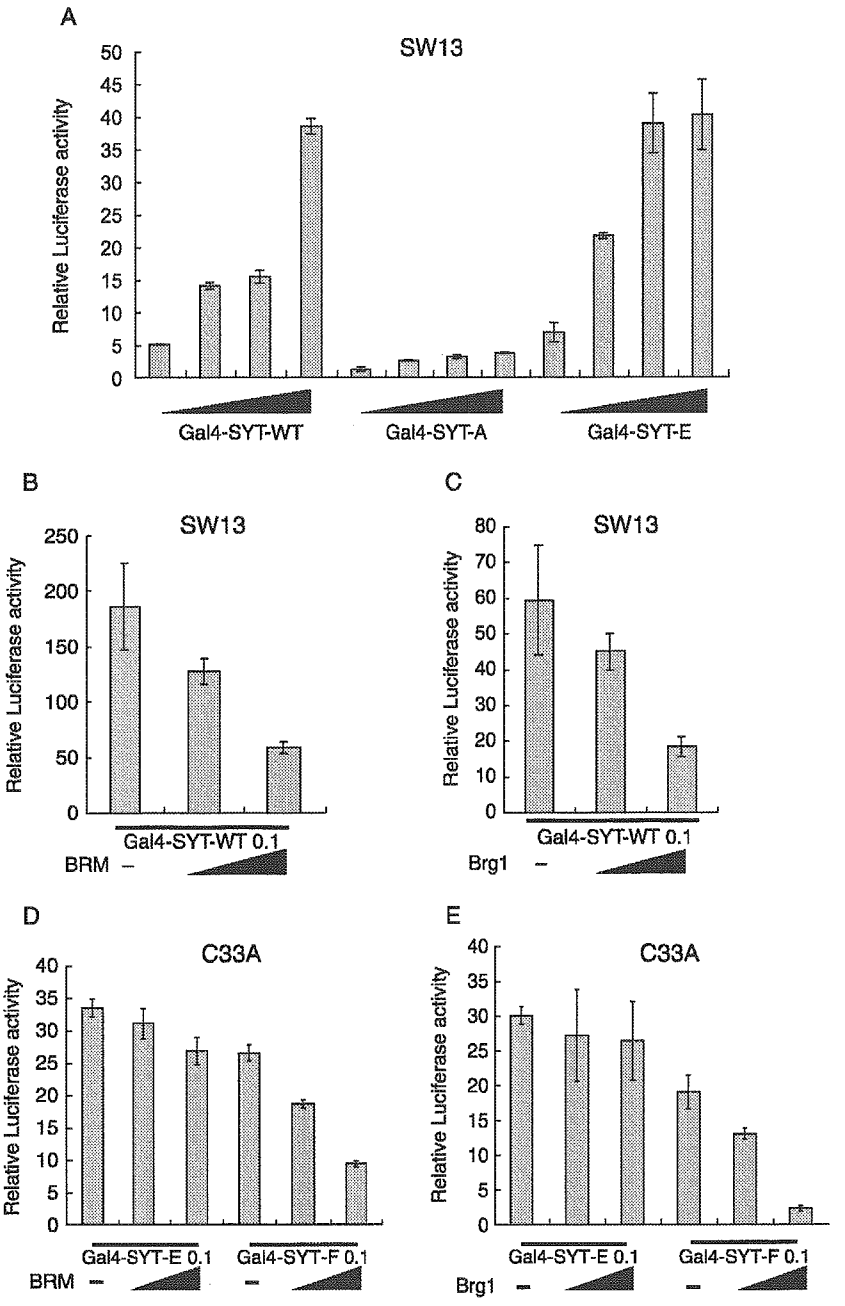

Figure 3 Analysis of the transcriptional co-activator activities of SYT using BRM- and Brg1-deficient cells. (A) The activities of the full-length SYT and its deletion mutants in the SW13 cell. The pG5luc reporter (0.25 μg) was co-transfected with increasing amounts (1 ng, 5 ng, 10 ng, 20 ng) of Gal4-SYT-WT, Gal4-SYT-A and Gal4-SYT-E in the SW13 cell that express undetectable levels of BRM and Brg1. (B, C) The SYT activity was repressed by addition of BRM or Brg1 in the SW13 cell. The pG5luc reporter (0.25 μg) was co-transfected with Gal4-SYT-WT (0.1 μg) in the SW13 cell. Increasing amounts (0, 0.1 and 0.5 μg) of BRM-pCIN or Brg1-pcDNA3.1 were co-transfected. (D, E) The repression of SYT activity by BRM and Brg1 was dependent on the N-terminal domain of SYT. The pG5luc reporter (0.25 μg) was co-transfected with Gal4-SYT-E (0.1 μg) and Gal4-SYT-F (0.1 μg) in C33A, the BRM/Brg1-deficient cell. Increasing amounts (0, 0.1 and 0.5 μg) of BRM (D) or Brg1 (E) expression vectors were co-transfected.

immunoprecipitated by anti-flag antibody M2-conjugated agarose, the bound proteins were washed and detected by anti-BRM or anti-Brg1 antibody. The cells were transfected with vector only (lanes 1 and 5), BRM (lane 2), BRM and flag-SYT-WT (lane 3), BRM and flag-SYT-D (lane 4), Brg1 (lane 6), Brg1 and flag-SYT-WT (lane 7) and, Brg1 and flag-SYT-D (lane 8). The amounts of expressed products of SYT-WT (lane 11) and SYT-D (lane 12) were detected by anti-flag antibody. (E) SYT protein co-localized with Brg1 and BRM in cultured cells. Panels a–d, GFP-SYT-WT and Brg1 were co-transfected in SW13 cell. Signals were detected by GFP autofluorescence (a), indirect immunofluorescence with anti-Brg1 antibody (b), overlay (c) and DAPI (d). Merged signals showed co-localization of SYT and Brg1 in nuclear speckles. Panel e–h; GFP-SYT-WT and BRM were co-transfected in SW13 cell. GFP-SYT-WT was detected by autofluorescence (e), indirect immunofluorescence with anti-BRM antibody (f), Overlay panel (g) and DAPI (h). BRM also co-localized with SYT in nuclear speckles, the same as Brg1.

regulates the SYT-WT activity in cultured cells. Next, to test whether BRM and Brg1 repress SYT transcriptional activity through the SYT N-terminal 70-amino acid domain that is the binding domain of BRM and Brg1, we analysed the activity of SYT-F in which the N-terminal 70 amino acids were fused to the SYT C-terminal transactivation domain (Fig. 1A) in SW13 and C33A cells. SYT-F transactivation activity was repressed by addition of BRM or Brg1, but that of SYT-E was not affected (Fig. 3D,E, and data not shown). These results suggest that BRM and Brg1 negatively regulate SYT transcriptional activity through their binding to the SYT N-terminal 70-amino acid domain.

BRM and Brg1 negatively regulate transcriptional activity of SYT using ATP-hydrolysis in SWI/SNF complexes containing BAF47b

It is known that BRM or Brg1 make SWI/SNF protein complexes with a lot of proteins. To examine whether repression by BRM or Brg1 is dependent on their protein complexes, we analysed the SYT-WT activity in the G401 cell that expresses undetectable levels of BAF47b, one of the subunits in the SWI/SNF complexes (Versteege *et al.* 1998; DeCristofaro *et al.* 1999, 2001). The transcriptional activity of SYT-WT was high, the same as that of SYT-E in the BAF47b-deficient cell (data not shown) as previously shown in the BRM- and Brg1-deficient cells, SW13 (Fig. 3A). The SYT-WT activity was repressed by the addition of BAF47b with dose dependency (Fig. 4A). This result suggests that BAF47b also works for the repression of the SYT activity and that BRM and Brg1 regulate SYT transcriptional activity in the SWI/SNF complexes.

It has been shown that BRM or Brg1 has ATPase activity, which is important for chromatin structure remodelling activity of SWI/SNF complexes (Vignali *et al.* 2000). To examine the effect of ATPase activity of BRM or Brg1 on the repression activity, we analysed the SYT-WT activity by addition of ATPase-deficient BRM or Brg1 in the SW13 cell. The SYT-WT transactivation was not repressed by addition of ATPase-deficient BRM or Brg1 (Fig. 4B,C). These results suggest that BRM and Brg1 may regulate SYT transcriptional activity using chromatin remodelling with ATP-hydrolysis in SWI/SNF complexes.

It is known that some of the SWI/SNF complexes contain HDAC (histone deacetylase) protein and show the repression activity for several gene transcriptions (Zhang *et al.* 2000; Kuzmichev *et al.* 2002). To examine whether the histone deacetylase activity has any effects on the SYT repression activity by BRM and Brg1, we analysed the SYT-WT activity by addition of TSA (trichostatin A), which is a histone deacetylase inhibitor, in SW13 cell. However, TSA has no effect on the repression (data not shown). This result indicates that repression of SYT activity by BRM or Brg1 was independent of the histone deacetylase activity.

Discussion

Recently, observations have revealed that SYT and BRM proteins are present in the same nuclear speckles and interact *in vitro* and *in vivo* (Thaete *et al.* 1999; Nagai *et al.* 2001). BRM is a component of human SWI/SNF complexes, which positively or negatively regulate transcriptions of several genes by chromatin structure remodelling activity (Vignali *et al.* 2000). We have confirmed this interaction and have newly demonstrated that Brg1, which is the BRM homologue and another component of SWI/SNF complexes, also interacts with SYT by using GST pull-down and co-immunoprecipitation experiments (Fig. 2B,C,D). These interactions were dependent on the N-terminal 70-amino acid residues of SYT. Furthermore, we have found that Brg1 co-localized with SYT in the nucleus of the cultured cell, the same as BRM (Fig. 2E).

As the SYT lacks obvious DNA binding domains, we analysed the activity of SYT using a luciferase reporter assay with fusing to the Gal4 DNA binding domain (Fig. 1). We have found that the activity of the full-length SYT is weaker than that of the N-terminal domain deleted mutant in the 293T cell (Fig. 1B), indicating that the activity of SYT was negatively regulated through its N-terminal domain in the 293T cell. Recently, it was shown that the SYT-SSX1 fusion protein has a colony-forming activity and the activity is suppressed by the over-expression of the SYT binding domain of BRM (Nagai *et al.* 2001). These findings led us to hypothesize that BRM or Brg1 may negatively regulate the SYT activity through its binding. Therefore, we analysed the activity of SYT in BRM- and Brg1-deficient cells (SW13 and C33A). The activity of the full-length SYT is strong, the same as the N-terminal domain deleted mutant in these cells (Fig. 3A, and data not shown), indicating that the N-terminal domain did not inhibit activity in BRM- and Brg1-deficient cells (SW13 and C33A). This indicates that BRM and Brg1 could be candidates for repressor of the activity of SYT. In these cells, we have found that the activity of the full-length SYT is repressed by addition of BRM and Brg1, but that of the N-terminal domain deleted mutant is not (Fig. 3B–E). These findings indicate that BRM and Brg1 negatively regulate SYT transcriptional activity through their binding to the SYT N-terminus.

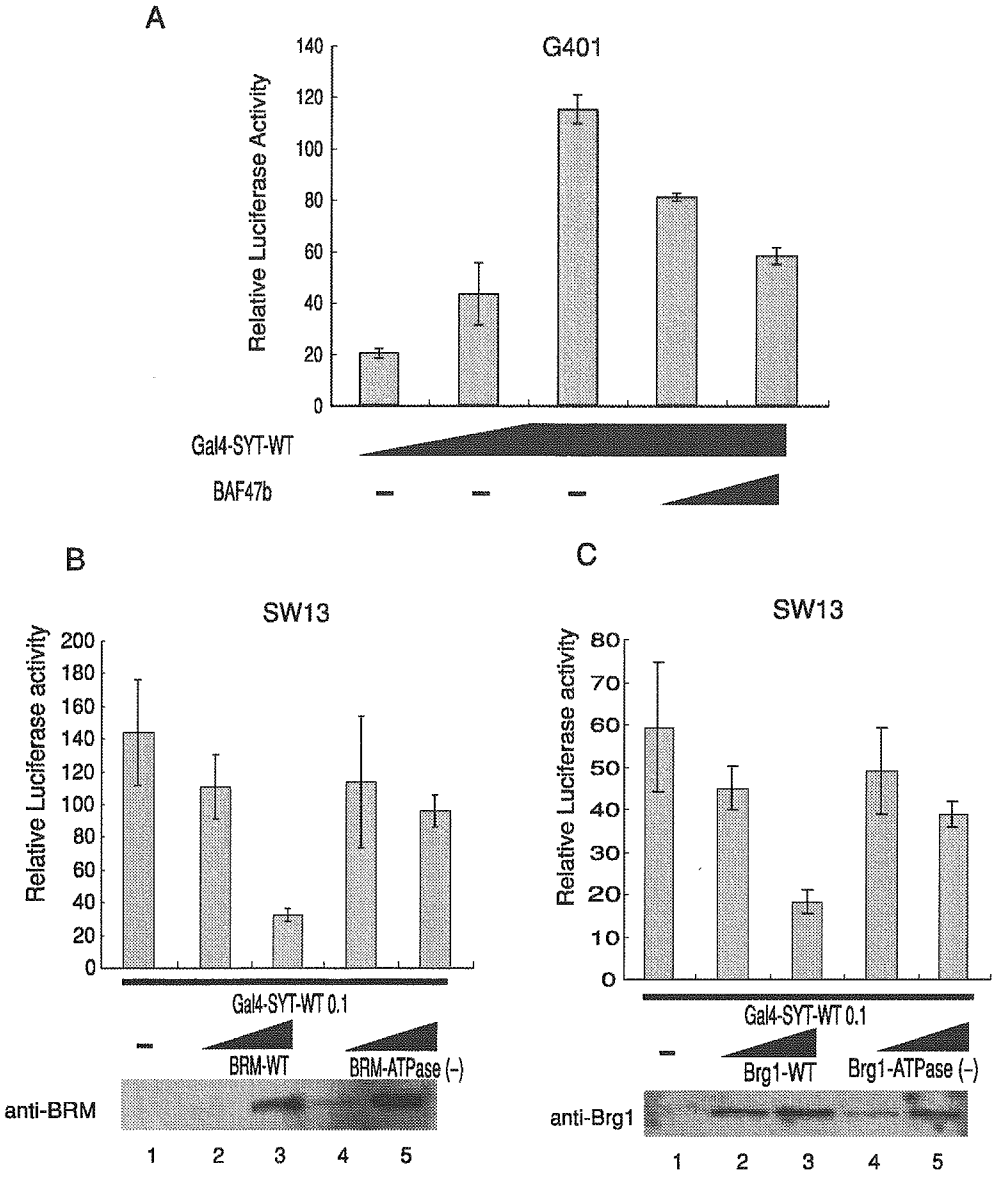

Figure 4 Repression of SYT transcriptional activity by BRM and Brg1 was dependent on BAF47b, which is another subunit of the SWI/SNF complexes, and on ATP-hydrolysis of BRM or Brg1. (A) SYT-WT has a strong transcriptional activity in the BAF47b-negative cell (G401) and the activity was repressed by addition of BAF47b. The pG5luc reporter (0.25 μg) was co-transfected with increasing amounts (0.01, 0.05 and 0.1 μg) of Gal4-SYT-WT in the G401 cell. BAF47b represses SYT transcriptional activity. The pG5luc reporter (0.25 μg) was co-transfected with Gal4-SYT-WT (0.1 μg) in the G401 cell. Increasing amounts (0, 0.01 and 0.1 μg) of BAF47b-pcDNA3.1 were co-transfected. (B, C) SYT transactivation activity was not repressed by ATP-hydrolysis-deficient mutants of BRM and Brg1. The pG5luc reporter (0.25 μg) was co-transfected with Gal4-SYT-WT (0.1 μg) in the SW13 cell. Increasing amounts (0.1 and 0.5 μg) of wild-type BRM (BRM-WT) and ATP-hydrolysis-deficient BRM [BRM-ATPase(–)] were co-transfected and the products of BRM-WT (lanes 2 and 3) and BRM-ATPase(–) (lanes 4 and 5) were detected by anti-BRM antibody (B). Increasing amounts (0.1 and 0.5 μg) of wild-type Brg1 (Brg1-WT) and ATP-hydrolysis deficient Brg1 [Brg1-ATPase(–)] were co-transfected, and the products of Brg1-WT (lanes 2 and 3) and Brg1-ATPase(–) (lanes 4 and 5) were detected by anti-Brg1 antibody (C).

The ATP-hydrolysis-dependent chromatin structure remodelling factors were originally described as the yeast SWI/SNF complex, which is composed of several subunits and positively regulates an HO gene (Stern *et al.* 1984). Human homologues of these subunits, which have an ATPase domain, have been identified as BRM and Brg1 (Khavari *et al.* 1993; Muchardt & Yaniv 1993). We have found that negative regulation of the activity

of SYT is needed for ATP hydrolysis of BRM or Brg1(Fig. 4B,C). Like this repression, it was shown that Brg1 negatively regulates the gene expression of cyclin-A and c-fos genes using ATP hydrolysis of Brg1 (Murphy *et al.* 1999; Strobeck *et al.* 2000). The repression of the cyclin-A gene by Brg1 was also dependent on HDAC activity (Zhang *et al.* 2000). We then analysed the effects of a histone deacetylase inhibitor TSA on the repression of the SYT activity by BRM and Brg1. However, TSA had no effect on the repression (data not shown). These results suggested that SWI/SNF complexes have at least two pathways to repress gene expression in dependence or independence on HDAC activity. We speculate that SWI/SNF complexes negatively regulate the transcriptional co-activator activity of SYT by recruiting transcriptional negative factors to the promoter, or by masking or changing the structure of the C-terminal active domain of SYT using ATP-hydrolysis energy.

Recently, it has been shown that SYT also interacts with a putative transcriptional factor AF10 through the N-terminal 90-amino acid residue of SYT, and with an acetyl transferase/transcriptional co-factor p300 through the N-terminal 250-amino acid residue of SYT (Eid *et al.* 2000; de Bruijn *et al.* 2001a). However these binding domains of SYT are overlapped, it is unknown whether these proteins interact together with SYT or compete for the binding. It has been shown that p300 interacts with SYT only during the G1 cell cycle phase (Eid *et al.* 2000), and that human SWI/SNF complexes are inactivated prior to chromosome condensation in the G2/M phase and re-activated during the G1 phase (Muchardt *et al.* 1996). These findings suggested that the transcriptional co-activator activity of SYT may be regulated in the cell cycle phase.

The BRM and Brg1 interacting region (amino acids 1–70) of SYT contains the so-called SYT N-terminal homology (SNH) domain (Fig. 1). Originally, the SNH was identified in EST sequences derived from a wide variety of species ranging from plants to human (Thaete *et al.* 1999). These EST sequences indicate that some of them are derived from SYT orthologs in mouse, rat, zebrafish and xenopus, while others are derived from novel SYT homologous genes from human, mouse and rat (Thaete *et al.* 1999; de Bruijn *et al.* 2001a). Two human genes of these homologues, SS18L1 and SS18L2, were mapped in chromosome 20q13.3 and 3p21, respectively. The SS18L1 protein has two functional domains; the N-terminal SNH domain and the C-terminal glycine, proline, glutamine and tyrosine-rich (QPGY) domain, the same as SYT, and has 63% sequence homology of SYT (Thaete *et al.* 1999; de Bruijn *et al.* 2001b). Recently, it was found that the SS18L1 gene was fused to the SSX1 gene in synovial sarcoma (Storlazzi *et al.* 2003). These findings may indicate that SS18L1 functions in normal tissue, the same as SYT, and the activity is regulated by BRM and Brg1 complexes. In contrast, the SS18L2 protein has the N-terminal SNH domain but not the C-terminal QPGY domain (Thaete *et al.* 1999; de Bruijn *et al.* 2001b), which is a transcriptional co-activator activity domain in SYT. This may indicate that the SS18L2 can bind to BRM and Brg1 and functions as a positive regulator (anti-repressor) of the transcriptional co-activator activity of SYT and SS18L1. A consensus tyrosine phosphorylation site was found in the SNH domains of SYT and its homologues (de Bruijn *et al.* 2001a). As tyrosine phosphorylation may play an important role in protein–protein interaction and protein trafficking (Pawson 1995), this conserved tyrosine phosphorylation site may serve to modulate the various interactions.

SYT is originally identified as a fusion partner to SSX1 in t(X;18) synovial sarcomas and AF10 is also identified as a fusion partner to MLL in t(10;11)-positive acute leukaemias. BAF47b, which is a subunit of the human SWI/SNF complexes, is known to be a susceptive gene in rhabdoid tumours (Versteege *et al.* 1998). Interaction of these proteins with SYT suggested that target genes of SYT may not only have implications for synovial sarcoma but also for development of other tumours. Therefore, it is important to find the target genes of SYT and to analyse the regulation of the genes by SYT through BRM, Brg1 and other binding proteins for understanding synovial sarcoma development.

Experimental procedures

Plasmid construction and antibodies

SYT mutant cDNAs fused to Gal4 DNA binding domain (DBD) were inserted in the *Eco*RI and *Hin*dIII sites of pCI-Neo (Promega) and pGEX23b (Amersham Pharmacia Biotech). Flag-tagged SYT mutants also are constructed with pCMV-Tag2 (Stratagene) without GAL4 DBD. The BRM cDNA was inserted in the *Eco*RI site of pCI-NEO and Brg1 was inserted in the *Bam*HI and *Xho*I sites of pcDNA3.1 (Invitrogen). The ATPase mutants of BRM (K751A) and Brg1 (K785A) were made by PCR, sequenced and inserted in pcDNA3.1. HA-tagged BRM and Brg1 were also constructed by inserting in pcDNA3.1. BAF47b cDNA was inserted in the *Bam*HI and *Sal*I sites of pcDNA3.1. pG5luc (Promega) contains five Gal4 binding sites and the adenovirus major late promoter upstream of firefly luciferase gene. pRL-TK (Promega) is used as a measure of transfection efficiency to normalize the firefly luciferase values. The GFP-SYT-WT expression vector was constructed by inserting in the *Kpn*I and *Not*I sites of pQBI 25-fC2 (Wako Chemical USA Inc.). Anti-Gal4 DBD antibody (Santa-Cruz, sc-577) and anti-flag antibody M2 (Sigma) were purchased.